MIKE
Powered by DHI

DHI Extended Oil Spill Model

Oil Spill Template

Scientific Description

DHI headquarters
Agern Allé 5
DK-2970 Hørsholm
Denmark

+45 4516 9200 Telephone
+45 4516 9333 Support
+45 4516 9292 Telefax

mike@dhigroup.com
www.mikepoweredbydhi.com

CONTENTS

DHI Extended Oil Spill Model
Oil Spill Template
Scientific Description

APPENDICES

1 Introduction / Feature Overview

An oil spill is the release of a liquid petroleum hydrocarbon into the environment. The oil may be a variety of materials, including crude oil, refined petroleum products (such as gasoline or diesel fuel) or by-products, ships' bunkers, oily refuse. During a well blow out a combination of gas and oil will be released under pressure and the MIKE OS model is capable of tracking both in the water column.

The model simulates the weathering and movement of oil and gas represented by discrete particles in a flow field utilizing the so-called Lagrangian approach. Dissolved oil is conveniently modelled using a coupled Eulerian model (MIKE 21/3 Advection-Dispersion module). The dissolved oil is automatically transferred to the coupled Eulerian model as dynamic point sources at each time step and the two models run in parallel during execution of the MIKE OS.

The model can handle surface spills and subsea oil / gas blow outs. Furthermore, it includes an advanced description of the effectiveness of emergency equipment (booms, skimmers, dispersants and in-situ burning)

The following environmental data are required for a MIKE 21/3 OS simulations:

- Current data in 2D or 3D. These will normally come from a coupled or de-coupled MIKE 21/3 FM simulation. The MIKE OS model may, however, utilize flow fields generated from third party software or other sources
- Wind data. These are used for calculation of the surface layer drift, Stoke's drift and e.g. the evaporation process.
- Wave data. These are used for the vertical dispersion of the oil.
- Ice data (optional).

The changes in chemical composition of oil residues over time is a result of physical and biological processes and is often referred to as 'weathering' of the oil. The oil is parameterized into three main oil fractions (volatile, semi-volatile, heavy), which is derived from the distillation curve of the oil, the content of wax and asphaltenes, and the density, viscosity and pour point – preferable as a function of degree of evaporation.

The weathering processes to be included in the simulations can be selected by the user, as most simulated weathering process can be separately enabled or disabled.

If needed, a "backtracking" of particles to determine the origin of spill can be performed using a time-reversed flow field provided by other tools of the Mike powered by DHI software.

Please note that the extended oil spill model template requires/utilises features currently only present in the MIKE FM series engines. Thus the advanced OS template can not be used with the classic NOIL engine (M21, M3, Cartesian grids).

2 What is Oil?

2.1 Introduction

Crude oil is a complex mixture of many chemical components. The relative compositions vary, resulting in many crude oil types with different chemical and physical properties.

The refinery distillation processes at an oil refinery converts the crude oil into a number of refined products, as shown in Figure 2.1 below.

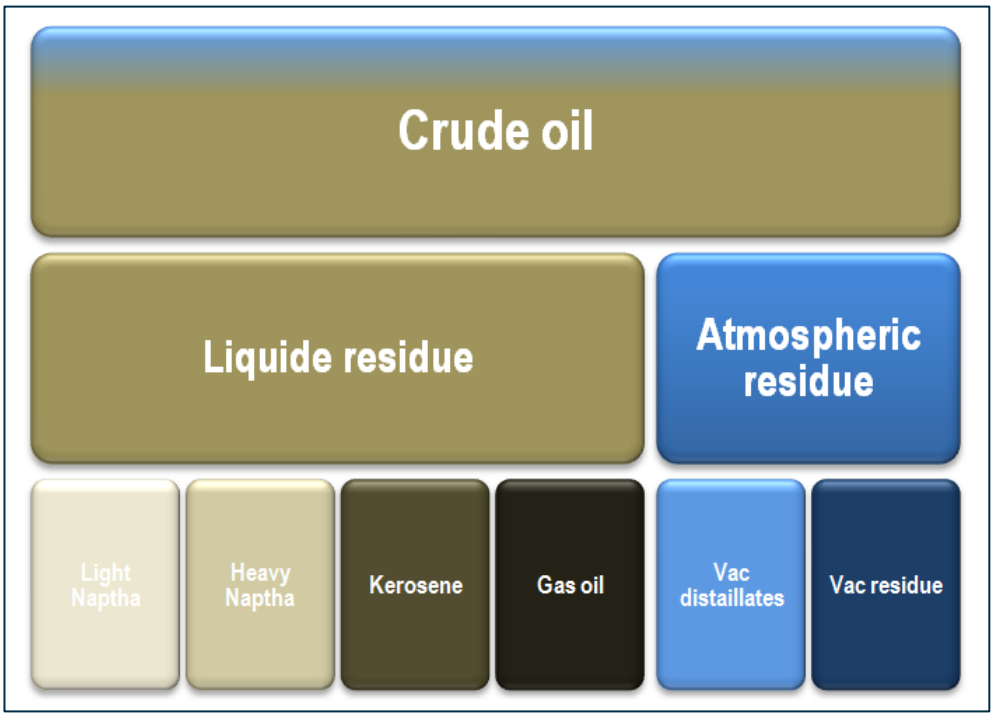

Figure 2.1 Conversion of crude oils into refined oil products by distillation

2.2 Oil components

For better prediction of the weathering processes the oil is often divided up into fractions or pseudo-components of certain properties. This usually requires detailed knowledge about the oil properties of each pseudo-component and its behaviour, where information like boiling point/vapour pressure and water solubility are important properties. Therefore, for modelling purposes it is required to find specific oil characteristics, either from a database or by performing additional calculations.

The oil spill templates used in the DHI oil weathering model describes the oil by three fractions: a light volatile fraction, a semi-volatile fraction and a heavy fraction. However, the vapour pressure/boiling point of each of the three fractions is allowed to change (decrease) as the lighter components have evaporated.

Each crude oil type has a different composition of the various components and it may be difficult to obtain the characteristics for the composition used in the DHI oil weathering model. If available, the distillation data will provide valuable information. In the model; the oil is divided into three oil fractions; a volatile fraction, a semi-volatile fraction and a heavy fraction. A minimum and a maximum boiling point, vapour pressure and water solubility is assigned to each of the three oil fractions. In addition, each fraction is assumed to biodegrade with different rates, thus each fraction is assigned a separate first order biodegradation rate constant.

Appendix A presents a more detailed description of how the oil is characterised and it presents examples on how to characterise and oil.

2.3 Weathering processes

Oil spilled on the water surface immediately spreads over a slick of few millimetres. The spreading is especially promoted by gravity and surface tension; however many spills of varying size quickly reach a similar average thickness of about 0.1 mm. Advection of currents and wind affects both surface oil and droplets dispersed in the water body.

Due to evaporation, emulsification, dispersion, dissolution, photooxidation, sedimentation and biodegradation the oil changes its physical and chemical properties and may disappear from the sea surface. All mentioned processes are dependent on each other and are referred to as oil weathering (see Figure 2.2).

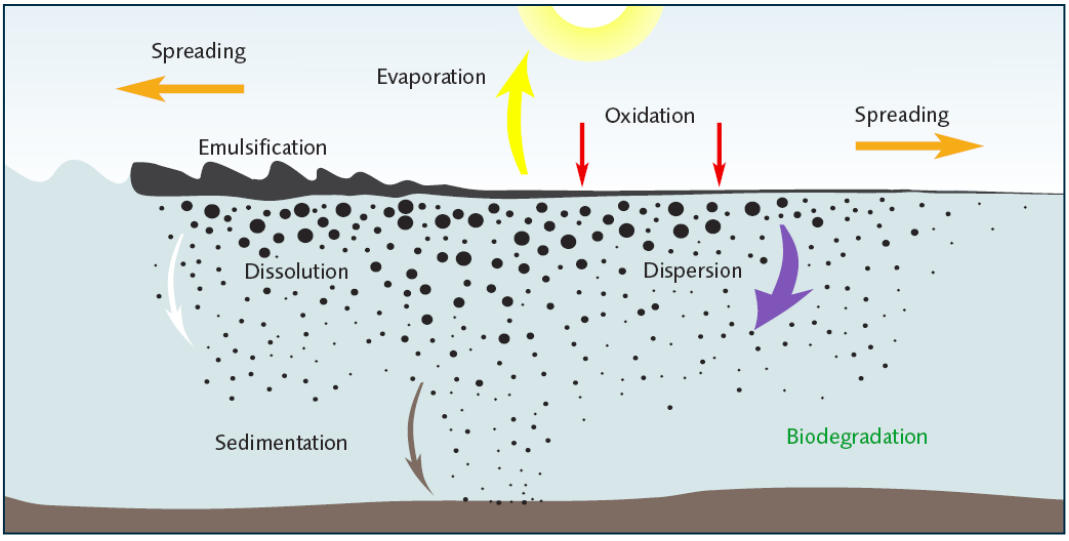

Figure 2.2 Processes acting on spilled oil (from ITOPF 2002)

During the lifetime of an oil spill the importance of different process for the weathering changes (Figure 2.2). Spreading, evaporation, dispersion and dissolution can be defined as short-term weathering processes, whereas emulsification, biodegradation and photochemical oxidation are recognised as long-term weathering processes.

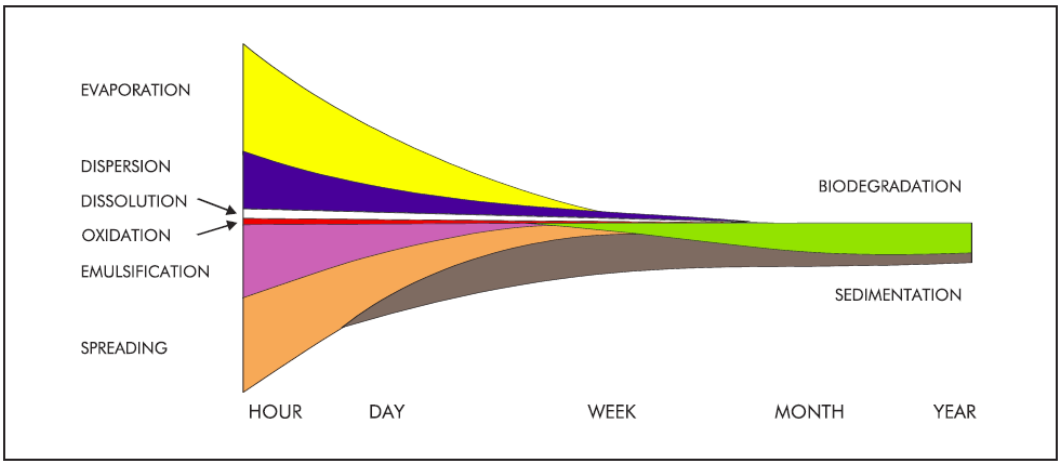

Figure 2.3 A schematic representation of the fate of a crude oil spill showing changes in the relative importance of weathering processes with time - the width of each band indicates the importance of the process (from ITOPF 2002)

The different chemical components in the oil are described, among other things, by the boiling point which is an indication of how volatile the component is and how it is affected by the weathering process. A schematic presentation of how these processes depend on each other and the oil components is given in Figure 2.4.

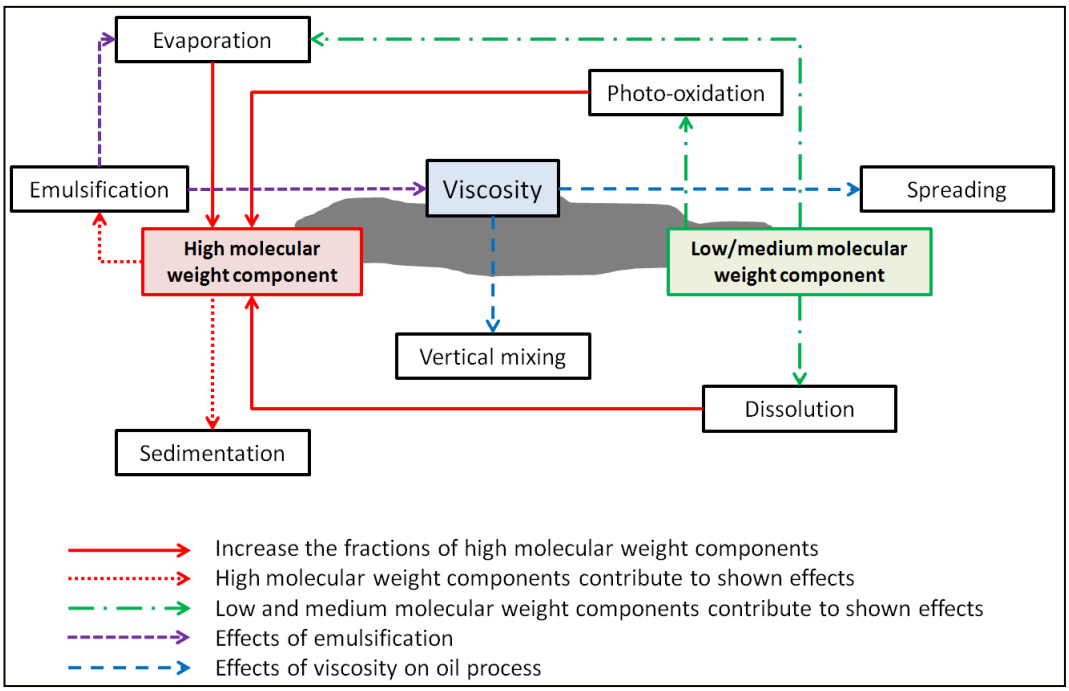

Figure 2.4 Effect of oil components and property on oil processes

3 Weathering Processes in the DHI Oil Spill Model

3.1 Weathering in the pseudo-component model

In general, the model describes the total amount of spilled oil as an assemblage of smaller oil amounts represented by individual oil particles. These individual oil particles are subject to weathering and drift process, working solely on the represented oil. Each particle is linked to some state variables, describing the changing of the associated oil fractions and other information.

As already described, the extended DHI oil spill model divides oil into three main fractions; a volatile fraction, a semi-volatile fraction and a heavy fraction that undergo detailed weathering and two conservative fractions (wax and asphaltenes). Also the water content is an important characterisation of the spilled oil as well as the represented surface area and the (average) depth.

Wax and asphaltenes components are considered as special fractions of the oil, and they are assumed not to degrade, evaporate or dissolve in the water. The content of wax and asphaltenes are important for the formation and stability of water-in-oil emulsions. The weathering of the other fractions is described in detail in the next sections as are the other state variables.

3.1.1 Volatile, semi-volatile and heavy oil masses

Each of the three fractions is subject to evaporation, dissolution, biodegradation and photooxidation.

The rate of change in oil mass is given as:

$$\frac{\mathrm{dOilmass_{VOLATILE}}}{\mathrm{dt}} = \begin{matrix} -\mathrm{EVAP_{VOLATILE}} \\ -\mathrm{DISS_{VOLATILE}} \\ -\mathrm{BIOD_{VOLATILE}} \\ -\mathrm{PHOT_{VOLATILE}} \end{matrix} \tag{3.1}$$

$$\frac{\mathrm{dOilmass_{SEMI-VOLATILE}}}{\mathrm{dt}} = \begin{matrix} -\mathrm{EVAP_{SEMI-VOLATILE}} \\ -\mathrm{DISS_{SEMI-VOLATILE}} \\ -\mathrm{BIOD_{SEMI-VOLATILE}} \\ -\mathrm{PHOT_{SEMI-VOLATILE}} \end{matrix} \tag{3.2}$$

$$\frac{\mathrm{dOilmass_{HEAVY}}}{\mathrm{dt}} = \begin{matrix} -\mathrm{EVAP_{HEAVY}} \\ -\mathrm{DISS_{HEAVY}} \\ -\mathrm{BIOD_{HEAVY}} \\ -\mathrm{PHOT_{HEAVY}} \end{matrix} \tag{3.3}$$

Where:

$EVAP_F$	evaporation of “F” fraction of oil, see section 3.2
$DISS_F$	dissolution of “F” fraction of oil, see section 3.3
$BIOD_F$	biodegradation of “F” fraction of oil, see section 3.5
$PHOT_F$	photooxidation of “F” fraction of oil, see Section 3.6
$_F$	refers to the oil fraction (VOLATILE, SEMI-VOLATILE, HEAVY)

3.1.2 Amount of asphaltenes

Asphaltenes are considered to be stable, i.e. the component does neither degrade, evaporate nor dissolve in water, thus the change in the amount of asphaltenes in an oil particles is set to zero:

$$\frac{\mathrm{dAsphaltenes}}{\mathrm{dt}} = 0 \tag{3.4}$$

3.1.3 Amount of wax

Wax components are also considered to be stable, i.e. the component does neither degrade, evaporate nor dissolve. Thus, the change in the amount of wax in an oil particle is set to zero:

$$\frac{\mathrm{dWax}}{\mathrm{dt}} = 0 \tag{3.5}$$

3.1.4 Water fraction of oil

Oil may readily take up water forming a water-in-oil emulsion.

The rate of change expression is given as:

$$\frac{dY_w}{dt} = +water_{uptake} - water_{release} \tag{3.6}$$

Where:

$water_{uptake}$	Uptake of water in oil (emulsification), see Section 3.4
$water_{release}$	Release of water from oil, see Section 3.4

3.1.5 Area of oil

This state variable is defined as the area of contact with the sea surface. It represents the equivalent area of a circular slick for the oil loading of an individual oil track particle. Please note that this area does not describe the total, by all particles covered area as an idealised, circular shape is assumed. Also this total covered area is not equivalent to the sum of all particle track areas as single particles can overlap. However, the sum of all particle track areas gives an upper bound for the total covered area. The current version of the oil spill model also includes a particle swarm spreading to avoid particle overlapping (see section 3.10) an a better approximation of the total area.

Fay defined three phases of the area spreading process: gravity–initial, gravity-viscous and surface tension–viscous spreading (Lehr, W.J., 2001).

The initial gravity phase is not described in the model. However, the initial area which has to be provided as model input correspond to the area at the end of the first phase and can be established from the following expression:

$$A_i = 3.4\pi \left(\frac{\Delta_w g V^5}{{\nu_w}^2} \right)^{1/6} \quad (3.7)$$

Where:

A_i	initial area of the oil particle at the start of the gravity-viscous phase [m^2]
Δ_w	relative oil-water density difference
V	volume of oil [m^3]
ν_w	water kinematic viscosity[m^2/s]

The area growth during the gravity – viscous spreading is described as:

$$A(t) = 2.1\pi \sqrt[3]{\frac{V^2 g \Delta_w \; t^{3/2}}{{\nu_{oil}}^{1/2}}} \quad (3.8)$$

Where:

A(t)	oil area as function of time [m^2]
ν_{oil}	oil emulsion kinematic viscosity [m^2/s]

The gravity-viscous spreading continue until a user specified minimum oil-thickness layer has been reached.

Spreading due to surface tension (wind shear) and/or currents is entirely handled by the Lagrangian spreading model.

3.1.6 Immersed state

The immersed state is used to separate oil particles that are in the water phase or stranded on the shore line. It will be '1' for a particle in the water phase and '0' for a particle not in the water phase.

If a simulated oil particle is thrown on land it may be absorbed (the position will be locked and no further movement is allowed) or reflected into the sea again. The probability of getting absorbed can be a single, global value or be specified as 2D map. See section 7 for details. Certain process will be only active if a track particle is immersed and not beached (i.e. area and water content change, dissolution and dispersion processes).

3.2 Evaporation

In the first hours and days of the spill, evaporation at the surface of the slick is the dominant weathering process (compare Figure 2.3). If the spill consists of a lightweight, highly refined product like gasoline, evaporation can very effectively remove nearly all of the spill contamination in as little as 24 hours. For spills of most medium-weight crudes the removal is less complete but substantial nevertheless. Typically, 10-30% of the material from these spills can be removed through evaporation in the first 24 hours.

Other factors effecting the evaporation of a spill include the amount of the spill exposed at the surface of the slick, wind and sea surface conditions.

The extended DHI oil spill model provides two possibilities to describe evaporation. After Fingas (1996, 1997) a simple time-dependent expression of the evaporation process may be used. A description of this is included in A.1. But most frequently, a more detailed modelling approach is applied. This is described in the below text.

The evaporation process for one particle that is in contact with the water surface (within 5 cm from surface) is calculated according to the 'Model of Reed', see Betancourt et al. (2005) and Reed (1989):

$$EVAP_F = \frac{K_F \cdot P_F^{sat} \cdot A(t)}{R \cdot T} \cdot MW_F \cdot f_F \quad (3.9)$$

Where:

K_F	Mass transfer coefficient is for fraction F [m/h]
P_F^{sat}	Vapour pressure of fraction F [atm.]
A(t)	Slick area of each particle in contact with water surface [m2]
R	Gas constant 8.206·10-5 atm m3/ mol K
T	Temperature [K]
f_F	fraction of oil fraction F
MW_F	Molecular weight of fraction F [g/mol]

The mass transfer coefficient is calculated according to Mackay et al. (1980) as:

$$K_F = 0.0292 \cdot U^{0.78} \cdot D^{-0.11} \cdot Sc_F^{-0.67} \cdot \sqrt{\frac{MW_F + 29}{MW_F}} \quad (3.10)$$

Where:

U	Wind speed [m/h]
Sc_F	Schmidt number for oil fraction F (dim.less)
D	Diameter of each particles area in contact with water surface [m]

The assumed diameter has a lower limit of 0.5 m for each particle and the minimum applied wind speed is 1m/h.

The Schmidt number, Sc, characterises the relative proportions of momentum and mass diffusion convection process. It can be interpreted as surface roughness information.

3.3 Dissolution from surface slick

Some part of the oil slick is removed as the water-soluble portion of the petroleum hydrocarbons are dissolved into the surrounding seawater. Although this reduces the size of the slick it presents an environmental problem since the water-soluble spill components and breakdown products are those that are most toxic to marine life. Small aromatic hydrocarbons like benzene and toluene, and somewhat larger polycyclic aromatic hydrocarbons (PAHs) like naphthalene, are among the water-soluble petroleum components known to have toxic effects.

Other factors affecting the dissolution of a spill include the amount of the spill exposed at the surface of the slick, wind and sea surface conditions, air temperature, and insolation intensity. Another factor is emulsification of the slick, which significantly retards the rate of evaporation.

The dissolution process for the oil fractions (F, F=volatile, semi-volatile, heavy) is calculated as:

$$DISS_F = k_{dis,F} \cdot A \cdot \frac{M_F}{M_{total}} \cdot \rho_F \cdot C_{W,F}^{sat} \quad (3.11)$$

Where:

$k_{dis,F}$	Dissolution rate for the oil fraction F (F=volatile, semi-volatile, heavy) [m/s]
M_F	Mass of oil fraction F in oil particle [kg]
ρ_F	Density of the oil fraction F [kg/m3]
A	Slick area of each particle in contact with water surface [m2]
$C_{W,F}^{sat}$	Water solubility of the oil fraction F[kg/kg]

3.4 Emulsification

Emulsification is the formation of a mixture of two distinct liquids, seawater and oil in the case of a marine spill. Fine oil droplets are suspended within (but not dissolved into) the water and the emulsification formed occupies a volume that can be up to four times that of the oil it originates from. Moreover, the viscous emulsion is considerably more long-lived within the environment than the source oil, and its formation slows subsequent weathering processes.

Emulsification tends to occur under conditions of strong winds and/or waves and generally not until an oil spill has persisted on the water for at least several hours. A persistent, partially emulsified mixture of water-in-oil is sometimes referred to as a 'mousse.' Mousse is resistant to biodegradation, the important final weathering stage, and in shallow marsh environments it can persist within sediments for years to decades.

The present model describes the emulsification as an equilibrium process between the two stages oil + water and water in oil. Stability of emulsions is an important factor determining ability of emulsions to demulsify, as unstable and meso-stable emulsions will release water. A first order water release formula is used to describe the process (Xie et al. 2007):

$$water_{uptake} = K_{em} \cdot (U+1)^2 \cdot \frac{Y_{max} - Y_w}{Y_{max}} \tag{3.12}$$

$$water_{release} = -\alpha \cdot Y_w \tag{3.13}$$

Where:

Y_w	water fraction [kg/kg]
Y_{max}	maximum water fraction [kg/kg]
U	wind speed [m/s]
K_{em}	emulsification rate constant. A typically of 2×10-6 s/m2 is given in Sebastião & Soares (1995).
α	water release rate, α=0 for stable emulsions; α>0 for meso-stable emulsions [s-1]

The water release rate α is related to the parameter for emulsion stability S.

$$\alpha = \begin{cases} \alpha_0 - \dfrac{(\alpha_0 - \alpha_{0.67}) \cdot S}{0.67} & S < 0.67 \\ \alpha_{0.67} \cdot \left[\dfrac{1.22 - S}{1.22 - 0.67}\right] & 0.67 \le S < 1.22 \\ 0 & S \ge 1.22 \end{cases} \tag{3.14}$$

Where:

α_0	water release rate for unstable emulsion with S=0.

It is set equal to $\ln\left(\frac{Y_{max}}{0.1}\right)/3600[s]$ corresponding to that the emulsion breaks down within a few hours at very low wind speeds.

$\alpha_{0.67}$ water release rate for the meso-stable emulsion with S=0.67.

It is set equal to: $\ln\left(\frac{Y_{max}}{0.1}\right)/(24 * 3600[s])$ corresponding to that a meso-stable emulsion breaks down within a few days at very low wind speeds.

In the oil spill model, the stability index formulated by Mackay and Zagorski (1982) is used:

$$S = X_a \cdot exp[K_{ao} \cdot (1 - X_a - X_w)^2 + K_{av} \cdot X_w^2] \cdot exp[-0.04 \cdot (T - 293)] \quad (3.15)$$

Where:

a	subscript represents asphaltenes
w	subscript represents wax
o	subscript represents other chemical components
K_{ao}	3.3 at 293 K
K_{aw}	200 at 293 K
X_a	fraction of asphaltenes
X_w	fraction of wax
T	temperature, K

Emulsions with S>1.22 are considered stable, whereas oils with a S value between 0.67 – 1.22 are considered to form meso-stable emulsions and oils with a S below 0.67 form unstable emulsion (Xie et al. 2007).

3.5 Biodegradation

Microbial oil degradation is a critical late-stage step in the natural weathering of petroleum spills, as it is the stage that gradually removes the last of the petroleum pollutants from the marine environment (compare Figure 2.3).

Microbial degradation of petroleum compounds occurs most rapidly via the oxidative metabolic pathways of the degrading organisms. As such, biodegradation is predicted to occur fastest in environments with ample oxygen as well as a diverse and healthy oil-degrading flora. Conversely, oxygen-depleted marine sediments that are often sites of petroleum contamination are among the habitats where aerobic metabolism is severely limited and microbial oil breakdown must therefore proceed via slower anaerobic pathways. Even though degradation within these sites is slow, it may still have a substantial cumulative impact over time.

The biodegradation process is calculated as a simple 1st order process:

$$BIOD_F = k_{bio,F} \cdot M_F \quad (3.16)$$

Where:

$k_{bio,F}$	Biodegradation rate for the oil fraction F[1/s]
M_F	Mass of oil fraction F in oil particle [kg]

3.6 Photooxidation

Chemical oxidation of the spilled oil also occurs, and this process is facilitated by exposure of the oil to sunlight. Oxidation contributes to the total water-soluble fraction of oil components. Less complete oxidation also contributes to the formation of persistent petroleum compounds called tars. The overall contribution of photooxidation to oil spill removal is small. Even exposed to strong sunlight (approximately 700 W/m2 in Europe), photooxidation only breaks down about a tenth of a percent (0.1%) of an exposed slick in a day.

The photooxidation process is calculated as a simple 1st order process:

$$PHOT_F = i \cdot k_{photo,F} \cdot M_F \tag{3.17}$$

Where:

$k_{photo,F}$	Photooxidation rate for the oil fraction F at sea surface[1/d] at a light intensity of 100 W/m²
M_F	Mass of oil fraction F in oil particle [kg]
i	Solar radiation at given distance from surface [normalised to 100 W/m2], calculated with Lambert Beer expression:

$$i = \frac{i_0}{100} \cdot e^{-\beta \cdot dsurf} \tag{3.18}$$

Where:

i_0	Solar radiation at surface [W/m2]
100	normalisation constant to 100 W/m²
β	Light extinction coefficient [1/m]
dsurf	Distance from particle to water surface [m]

3.7 Vertical dispersion by wave action

An important factor moving the oil into the water column is vertical dispersion. Strong winds, currents, and turbulent seas facilitate the process of dispersion.

Breaking waves cause the oil droplets to be moved far into the water column. This is by far the most important dispersion mechanism. The modelling of the entrainment of oil from the sea surface into the water column is based on Johansen et al. (2015):

$$\mathrm{Q_d} = -\beta * Q_S \tag{3.19}$$

Where:

Q_d	is the net amount of oil dispersed in a time step
Q_S	is the amount of oil on sea surface
β	is a first order rate constant calculated by

$$\beta = \mathrm{P} * \frac{WCC}{T_m} \tag{3.20}$$

Where:

P^*	is here set to the fraction of the oil which has not re-dispersed within the time-step used in the calculations (dt)

T_m	is the mean wave period
WCC	is white cap coverage

The white cap coverage is calculated as:

$$\begin{aligned} &WCC = 0;\ U_w < 3.7\ m/s \\ &WCC = 3.18 \cdot 10^{-5} \cdot (U_w - 3.7)^3; 3.7 < U_w < 11.25 \frac{m}{s} \\ &WCC = 4.82 \cdot 10^{-6} \cdot (U_w + 1.98)^3; 9.25 < U_w < 23.1 \end{aligned} \quad (3.21)$$

Where:

U_w	wind speed [m/s]

The oil will be dispersed into the water column as oil droplets with different sizes. The sizes of these droplet diameters are very dependent on the wave action and inherent oil properties like viscosity, density and water-oil interfacial tension.

The number averaged droplet diameter $d_{50,N}$ is calculated according to Johansen et al. (2015) as:

$$\frac{d_{50,N}}{h} = A \cdot We^{-\alpha} \cdot \left[1 + \frac{B}{A} \cdot \left(\frac{We}{Re}\right)^{\alpha}\right] \equiv A \cdot We^{-\alpha} \cdot [1 + B' \cdot (Vi)^{\alpha}] \quad (3.22)$$

Where

$d_{50,N}$	is the number averaged diameter

$$Vi = \frac{We}{Re} = \frac{\mu \cdot U_H}{\sigma}$$

$$B' = \frac{B}{A}$$

$$We = \frac{h \cdot \rho \cdot U_H^2}{\sigma}$$

$$Re = \frac{h \cdot \rho \cdot U_H}{\mu}$$

h	is the surface oil film thickness (m)
H	wave amplitude or free fall height (m)
U_H	is the free fall velocity = $\sqrt{2 \cdot g \cdot H}$
μ	is the oil dynamic viscosity (kg /(m·s))
ρ	is the oil density (kg/m3)
g	is the acceleration of gravity (9.81 m/s2)
σ	is the interfacial tension (N/m)
U	is the wind speed at 10m height
α	is a coefficient calculated to 0.6 from measured data

A =2.251	(derived from measured data)
B' = 0.027	(=>B = 0.027×2.251 = 0.061) (derived from measured data)

The volume average diameter, $d_{50,V}$, is calculated from $d_{50,N}$:

$$\log_{10}(d50, v) = \log_{10}(d50, n) + 3 * S_2 \quad (3.23)$$

where S is the logarithmic standard deviation, found to be about S=0.38 (Johansen et al. 2015).

The droplet size distributions are assumed to follow the Rosin-Rammler-type distribution:

$$f_{v(d)} = 1 - e^{-c*\left(\frac{d}{d_{50,N}}\right)^{1.8}} ; c = 0.693 \quad (3.24)$$

Where

$f_V(d)$ is the volume fraction having a diameter below d

P* is found by combining Stokes Law with the above expression for the oil droplet size distribution:

$$P^* = 1 - e^{-c*\left(\frac{d_{crit}}{d_{50,N}}\right)^{1.8}} \quad (3.25)$$

Where:

d_{crit} is defined as the diameter of smallest droplet re-surfacing within the time-step used in the calculations. It is calculated from Stokes equation:

$$\mathrm{d_{crit}} = \sqrt{\frac{\mathrm{H_t}}{\mathrm{dt} \cdot \mathrm{K^s}}} \quad (3.26)$$

Where

$$\mathrm{K^S} = \frac{(\rho^{\mathrm{water}} - \rho^{\mathrm{oil}}) \cdot \mathrm{g}}{18 \cdot \eta^{\mathrm{water}}} \quad (3.27)$$

Where

ρ^{water} is the water density [kg/m^3]
ρ^{oil} is the oil density [kg/m^3]
η^{water} is the water viscosity [kg/m/s]
dt is the time step
g is the acceleration of gravity [9.81 m/s^2]
H_t is the entrainment depth [m]

The entrainment depth, H_t, is according to Delvigne and Sweeney (1988) calculated by:

$$\mathrm{H_t} = (1.5 \pm 0.35) \cdot \mathrm{H_b} \quad (3.28)$$

Where:

H_b breaking wave height ≈1.67*Hs

The probability of individual particles to disperse vertically due to wave breaking is determined as:

$$\mathrm{p_{wbreak}} = \mathrm{Min}\left(1, \frac{\mathrm{Q_d}}{\mathrm{M_{Total}}}\right) \quad (3.29)$$

Where:

M_{Total} Total oil mass of the particle.

If a particle becomes dispersed the distance that the oil droplets are dispersed into the water column. This distance *disp*$_{wbreak}$ is determined by a standard normal distribution N (μ, σ^2)

$$\mathrm{disp}_{\mathrm{wbreak}} = \mathrm{N}(\mu, \sigma^2) \tag{3.30}$$

Where:

μ	average depth ≈ 1.5 * Hb
σ^2	standard deviation ≈ 0.35 * H_b

3.7.1 Dissolution of dispersed oil droplets in the water column

Usually the oil density is smaller than the water density. The dispersed oil droplets therefore tend to resurface. However, they can remain dispersed for a long time, due to water turbulence and they may be dissolved before reaching the sea surface again.

The vertical movement of the oil droplets is driven by buoyancy forces from differences in oil density and water density in both upward and downward direction. The implementation is based on Stokes Law as described in section 3.8.

Assuming - as for the dissolution from surface oil slick – that the dissolution is proportional to the droplet surface, the change in droplet diameter with time can be expressed by:

$$\mathrm{d}(\mathrm{t}) = \mathrm{d}_0 - \mathrm{k}' \cdot \mathrm{t} \tag{3.31}$$

Where

k’	is an overall dissolution rate constant calculated from: $\mathrm{k}' = 2 \cdot \mathrm{k}^{\mathrm{dissol}} \cdot \mathrm{C}_{\mathrm{w}}^{\mathrm{sat}}$
k^{dissol}	dissolution rate constant (m/d) – the equation used for the calculations are basically the same is used for the dissolution from surface slick see section 3.3. However, to ease the calculations an average, overall k_{dissol} is used.
C_w^{sat}	water solubility (kg/kg)
d	droplet diameter (m)
d_0	initial droplet diameter (m)

This leads to the below expression of the dissolution rate from the dispersed oil droplets:

$$\text{Dissolution rate } (\frac{\mathrm{m}^3}{\mathrm{s}}) = \mathrm{N}_{\mathrm{droplets}} \cdot \frac{\pi}{2} \cdot \mathrm{d}^2 \cdot \mathrm{k}' \tag{3.32}$$

3.8 Sedimentation

Very few crudes have a density above the density of sea water, so only few will sink on their own in seawater. A few crudes may weather so much that the density of the residue become higher than the density of the seawater. Ignition of the oil may also result in a residue with a density above the seawater density.

The model can however handle the oils vertical movement driven by buoyancy forces due to the differences in oil density and water density in both upward and downward direction. The implementation is based on minor modifications of the expressions in Li Zheng, Poojitha D. Yapa (2000). These expressions are quite complex and appendix 0 gives further details.

3.9 Subsea blow-out

All above processes refer mainly to an oil spill on the sea surface. However, DHI's oil spill model does also include the option of simulating a subsea blow out. A subsea blow-out is simulated by modelling the rising of the plume utilizing an appropriate jet description. In MIKE OS the jet description itself is based on Jirka, G.H. (2004). The plume is described via the particles being emitted throughout the duration of the subsea blow-out. However, the position of the particles is determined by solving the equations by Jirka at each time step. The jet solution require time steps being only a fraction of the time step used in the Lagrangian drift model. For that reason the simulations are computed in a standalone model (a DLL) integrated into the MIKE ECO Lab model and all being a part of the MIKE OS. Once the particles in the plume become neutral buoyant with the ambient flow or the momentum in the jet is "small" the particles are "released" from the plume and further drift is handled in the Lagrangian drift model.

The plume at any position is characterised by a plume radius (bk) and a height (hk) – see Figure 3.1.

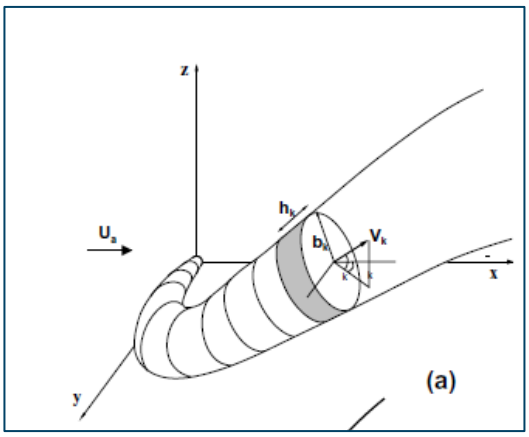

Figure 3.1 Schematic drawing for a buoyant jet. From Lee et al. (2000)

The plume will consist of different components: Gas/gas hydrates, oil droplets and water.

Several parameters and processes need to be considered for the simulation of the transport and fate of the buoyant jet:

Rising velocity

The difference in plume density and ambient density drives the buoyancy of the plume. The density of the plume will change significantly during the vertical rising, both due to the decrease in ambient pressure and due the processes going on during the rising. In addition to the differences in densities, the size of the bubbles (see appendix C.1.2) and the vertical velocity (see appendix C.2) and the oil droplets sizes (see appendix C.1.1) are of importance for the calculation of the rising velocity.

Plume

- Entrainment of water
- Bending of the plume, which is calculated in dependence of the currents

Gas

- Gas leakage due to the bending of the plume
- Decrease in molar volume with decreasing depth
- Dissolution of gas from the plume into the ambient water (see appendix C.3.2 and C.3.3 for details on the calculation of the dissolution rate of the gas)
- Formation/disintegration of hydrates

Oil

- Dissolution of oil components into ambient water (see appendix C.3.1 for details on the calculation of the dissolution rate)

3.9.1 Plume density

During the vertical rising, the plume density will change – both due to above listed processes during the rising of the plume.

The density of the plume is calculated from:

$$\rho_{Plume} = \frac{M_{Plume}}{V_{Plume}} \tag{3.33}$$

Where

$$M_{Plume} = \frac{G \cdot MW_G}{1000} + M_1 + M_2 + M_3 + PW + (MW_G + n_H \cdot MW_{PW}) \cdot \frac{G_H}{1000} \tag{3.34}$$

$$V_{Plume} = G \cdot V_G + \frac{M_1}{\rho_1} + \frac{M_2}{\rho_2} + \frac{M_3}{\rho_3} + \frac{PW}{\rho_{PW}} + \frac{MW_G + n_H \cdot MW_{PW}}{\rho_{hydrate}} \cdot \frac{G_H}{1000} \tag{3.35}$$

Where

G	is the number of “free” gas molecules (moles)
G_H	is the number of gas molecules caught in a hydrate (moles)
MW_G	is the molar mass of gas (g/mole)
V_G	is the molar volume of the gas
ρ_F	is the density of oil fraction F (F = VOLATILE, SEMI-VOLATILE, HEAVY) (kg/m^3)
ρ_{PW}	is the density of water (kg/m^3) (=ρ_a the density of the ambient water)
$\rho_{hydrate}$	is the density of hydrate (kg/m^3)
n_H	is no of moles water around one mole gas (depends on type of gas)

3.9.2 Gas density

In deep water with high pressures, gas does not behave as an ideal gas. The PVT-relationship for a gas may be described as:

$$Zc = \frac{P \cdot V}{R \cdot T} \tag{3.36}$$

Where

P	is the ambient pressure (Pa) = 101325 Pa + [Depth·Water density·g]
V	is the molar volume (m^3/mole)
T	is the ambient absolute temperature (K)
Zc	is the so-called compressibility factor, being equal to 1 if an ideal gas.

Several methods exist for calculating Z. The Pitzer equation is used in the DHI's Oil Spill:

$$Zc = 1 + \frac{B \cdot P}{R \cdot T} = 1 + \frac{B \cdot P_C}{R \cdot T_C} \cdot \frac{P_r}{T_r} \tag{3.37}$$

Where

P_C	is the critical pressure for the gas
T_C	is the critical temperature for the gas
P_r	is the reduced pressure = P/PC
T_r	is the reduced temperature = T/TC

Details on the parameters entering the Pitzer equation are given in Appendix C.4.

$$V_G = \frac{R \cdot T}{P} \cdot [1 + \{\left(0.083 - \frac{0.422}{T_r^{1.6}}\right) + \omega \cdot \left(0.139 - \frac{0.172}{T_r^{4.2}}\right)\} \cdot \frac{P_r}{T_r}] \tag{3.38}$$

The gas density (ρ_G) (kg/m^3) can then be calculated by

$$\rho_G = \frac{P \cdot M_{WG}}{Zc \cdot R \cdot T \cdot 1000} \tag{3.39}$$

See Appendix C.4 for further details on the calculation of the gas density.

3.9.3 Water entrainment

Proper estimation of the entrainment is important as it has a great impact on the density and thus the buoyancy of the plume. CDOG calculates the water entrainment. CDOG applies a quite advanced model developed by Lee et al. (1990). The same equations are applied in DHI's oil spill model.

The forced entrainment is computed as a sum of shear-induced entrainment and forced entrainment. The latter is computed based on the ambient flow interception in the windward side of the buoyant plume.

More details on the applied equations are provided in Appendix C.6.

3.9.4 Gas leakage

If the plume bents then the vertical rising gas bubbles may be released from the plume. Gas escaping the plume may happen if the plume is bent over by the cross-current (see Figure 3.2) as gas bubbles have a higher individual rise velocity than the plume. The amount of gas escaping the plume is calculated from the velocity component of the gas normal to the velocity of the plume. If the velocity is larger than the rate of increase in plume radius then an amount of gas is simulated to escape the plume.

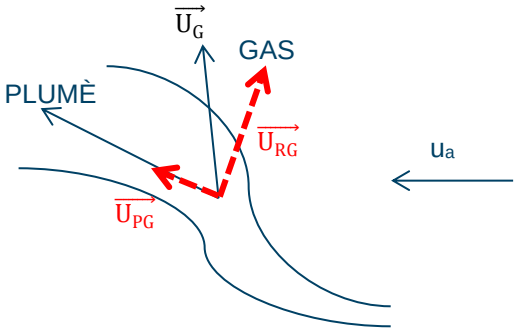

Figure 3.2 Gas may escape as angle is more steep than the plume angle

Criteria for that gas may leak (all three criteria should be fulfilled):

- the vertical distance travelled by the plume (z) should be above a critical distance, Z_{sm}, which is calculated from current velocity, initial linear velocity of plume, and leakage rate of gas and oil
- The angle (measured from a horizontal plane) at which the gas will move immediately after escaping from the main plume shall be steeper than the angle of plume
- The gas velocity normal to the plume direction (U_{RG}) so be larger the rate with which the radius of the plume increases

Appendix C.7 describes the equations applied for the calculation of the gas leakage.

DHI's Oil Spill model has included a module (Gas Module) simulating the fate and transport of gas bubbles once the gas bubbles have been released to the ambient water – see appendix D for further details. This module includes the modelling of the gas dissolution into water and the changes in molar volume and density with depth.

3.9.5 Formation and disintegration of gas hydrates

Formation and decomposition of gas-hydrates may take place within a range of P(ressure)-T(emperature) conditions. The program checks if a gas-hydrate can exist at the prevailing conditions. If so, then the formation of gas hydrates is described by a simple equation:

$$\frac{dG}{dt}_{Gas\ consumed} = -G \cdot K_f \cdot A_{Hyd} \cdot \left(f^{dissolution} - f^{equilibrium}\right) \quad (3.40)$$

Where

A_{Hyd}	is the surface area of a mole of empty gas hydrates [m^2]
$f^{dissolution}$	is the fugacity of the gas in dissolution [Pa]
$f^{equilibrium}$	is the fugacity of the gas at equilibrium [Pa]
K_f	is a rate constant for the formation of hydrates [$1/m^2/d/Pa$]

If the P-T conditions are so that gas hydrates do not exist at equilibrium, and if gas hydrates have been formed within the plume, then the decomposition of the gas hydrates is described by:

$$\left(\frac{dG_H}{dt}\right)_{\text{Gas released}} = -G_H \cdot K_d \cdot A_{Hyd} \cdot \left(0 - f^{dissolution}\right) \quad (3.41)$$

K_d is a rate constant for the decomposition of hydrate [$1/m^2/d/Pa$]

It is assumed that the gas released from a hydrate is immediately dissolved in the ambient water.

More details on the applied equations are provided in Appendix C.5.

3.9.6 Heat balance

A heat balance for the calculation of the plume temperature is included. The heat capacity of the oil fractions and ambient water together with the latent heat of hydrate formation and disintegration is used for the calculations of the temperature.

More details on the applied equations are provided in Appendix C.8.

3.10 Particle swarm spreading / non-overlapping movement

The oil spill template can simulate the spreading of oil with two different mechanisms. Apart from the gravity/ surface tension caused spreading of the oil (i.e. the surface area change of the individual oil parcel represented by each Lagrangian particle, see 3.1.5) a second mechanism ensures that oil particles do not overlap on the surface.

This mechanism moves particles at the water surface away from each other when an overlap is detected. It utilises some of the underlying features of the DHI ABM engine core to find neighbourhood relations between the particles. The basic principle is shown in the sketch below.

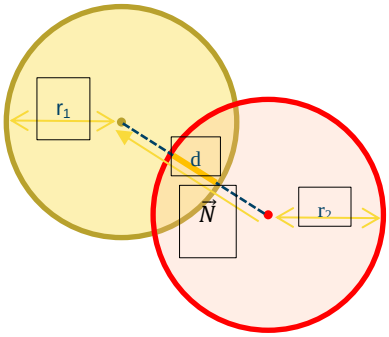

Here the “red” particle with the radius r_2 detects an overlap with the other particle (radius r_1) by calculating the distance d (=$|\vec{N}|$) between the centres. The overlap ***o*** is now $o = -(d - r_1 - r_2)$

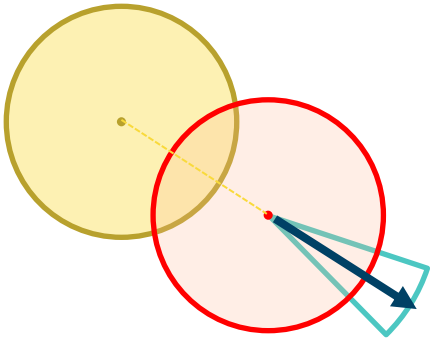

If an overlap is detected (i.e. ***o>0***) the red particle is moved away from the other particle with a speed that is proportional to the overlap size. The direction is opposite to the direct angle towards the centre of the other particle ($\measuredangle\vec{N} + 180° \pm 15°$)

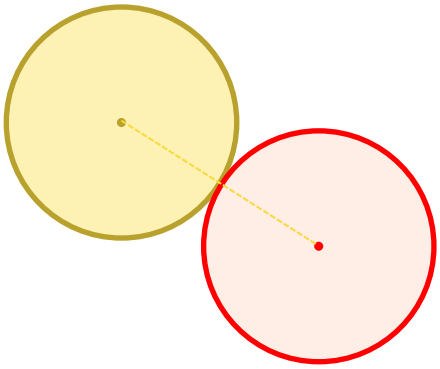

Final resulting particle positions

Note:
The computation of the nearest neighbour and the overlap checking is connected to high computational costs but can lead to a significant better approximation of the oil slick geometry/distribution.

3.11 Physical properties of oil

The term oil describes a broad range of hydrocarbon-based substances. Hydrocarbons are chemical compounds composed of the elements hydrogen and carbon. This includes substances that are commonly thought of as oils, such as crude oil and refined petroleum products, but it also includes animal fats, vegetable oils, and other non-petroleum oils. Each type of oil has distinct physical and chemical properties. These properties affect the way oil will spread and break down, the hazard it may pose to aquatic and human life, and the likelihood that it will pose a threat to natural and man-made resources.

3.11.1 Dynamics of viscosity

The oil viscosity will increase during weather due to evaporation of the most volatile fractions and due to uptake of water.

The change in parent viscosity due to removal of the most volatile fractions is modelled through the equation:

$$\mu_{oil} = \exp\left[B_{viscocity} \cdot f_w + C_{viscocity}\right] \tag{3.42}$$

Where:

μ_{oil}	inherent oil viscosity [cP].
f_W	evaporated fraction (weight)
$A_{viscosity}$	parameter determined from oil property data
$B_{viscosity}$	parameter determined from oil property data
$C_{viscosity}$	parameter determined from oil property data

The parent viscosity μ_0 is subsequently temperature corrected. In the model a simple exponential temperature dependency is assumed:

$$\mu_0 = \frac{\mu_{oil}}{\exp(b \cdot T/T_{ref})} \tag{3.43}$$

Where:

b	coefficient for temperature dependency [1/°C]
T	Temperature [°C]
μ_{ref}	oil viscosity [cP] at given reference temperature.
T_{ref}	reference temperature [°C]

Change in viscosity as a result of emulsification can be calculated using the Mooney equation, Sebastião and Guedes Soares (1995):

$$\mu = \mu_o \cdot exp\left[\frac{2.5 \cdot Y_w}{1 - C_1 \cdot Y_w}\right] \tag{3.44}$$

Where:

μ_{oil}	parent oil viscosity [cP].
C_1	viscosity constant (“Mooney constant”), final fraction of water content, 0.7 for crude oil and heavy fuel oil, 0.25 for home heating oil
Y_w	water fraction [kg/kg]

3.11.2 Dynamics of density

The physico-chemical properties of oil also vary with the temperature, and the fluid dynamics are therefore strongly temperature dependent. As the temperature of the spilled oil is typically above the pour point immediately after the spill, the density is rather low, making the oil buoyant and therefore the oil slick is forced towards the water surface in the beginning. However as the oil slick cools down, the density increases and minimises the density difference to the enclosing water, and therefore the slick can react to turbulent waters by dispersing under the surface.

The temperature dependency of the fluid density is based on the volumetric thermal expansion of a fluid:

$$\rho_T = \frac{\rho_0}{1 + \beta \cdot (T - T_0)} \tag{3.45}$$

Where:

ρ_T	final density [kg/m3]
T	temperature [°C]
ρ_0	reference density [kg/m3]
T_0	reference temperature [°C]
β	volumetric temperature expansion coefficient [1/°C]

It is assumed that the density of sea water is correctly given in the model inputs. The initial density for the light and heavy oil fraction has to be given at 20°C and is corrected to the ambient temperature using the above formula. The expansion coefficients for the fractions can be parameterised independently. Table 3.1 lists some generic values for common fluids.

Table 3.1 Example of volumetric temperature expansion coefficients for various liquids

Liquid	Volumetric temperature expansion coefficient [1/°C]
Water	0.00018
Petroleum	0.001
Oil	0.0007
Kerosene, Gasoline	0.001

As a result of emulsification and temperature the density of oil slick changes. The general density of the emulsion is calculated as:

$$\rho_e = Y_w \cdot \rho_w + (1 - Y_w) \cdot \rho_o \tag{3.46}$$

Where:

ρ_e	emulsion density [kg/m3]
ρ_w	seawater density [kg/m3]
ρ_c	oil density [kg/m3]
Y_w	water content

The oil density is calculated as

$$\rho_o = \frac{M_{total}}{\sum_{i=1}^{i=5} \frac{M_i}{\rho_i}} \tag{3.47}$$

Where:

ρ_o	oil density [kg/m3]
ρ_i	density of oil component i (i=1-5:volatile, semi-volatile, heavy, asphaltenes, wax) [kg/m3]
M_i	Mass of oil component i [kg]

4 Mechanical oil recovery using Booms and Skimmers

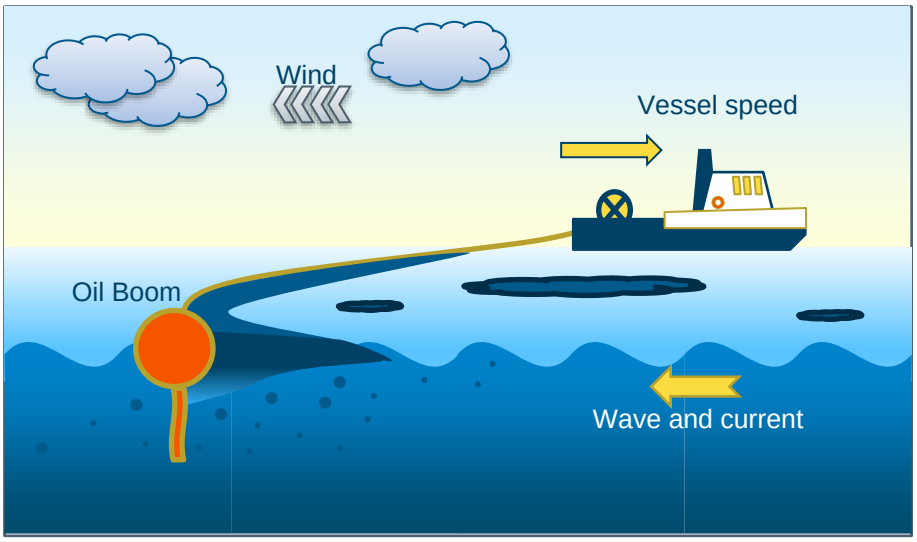

Figure 4.1 Sketch of mechanical oil cleaning and factors affecting its efficiency

The efficiency of mechanical recovery is highly dependent on the selected equipment, the oil properties, the weather conditions and the speed of the towing vessels (Figure 4.1). The dynamic positioning of equipment and specification of potential pumping capacity and towing speed is introduced using the MIKE Oil Spill toolbox. When specifying the potential pumping capacity it is strongly advised (Norsk Olje og Gass (2013) and Nordvik, A. B. (1999)) to consider the implication of

- Cleaning
- Repositioning
- Connection, emptying and transit to deliver recovered oil
- Re-positioning of finding oil slicks
- Personnel replacement and re-supplying ship

Oil may drift under the oil boom skirt or it may splash over the boom.

In the present context, the term leakage is used when then the equipment cannot pick up the oil for some reason. In the same way, the pumping efficiency may be reduced due to oil properties or other conditions as discussed below:

At any time step the probability of boom leakage and hence actual efficiency is evaluated as follows:

4.1 Factors impacting efficiency

4.1.1 Effect of wind

The leakage probability is equal to 100 % at wind speeds larger than a user specified threshold level W_{max}. According to Norsk Olje og Gass 2013, most operations stops and

the oil will to a large extend be naturally dispersed into the water column at wind speeds larger than 14 m/s.

4.1.2 Effect of waves

According to Norsk Olje og Gass 2013, an efficiency reduction factor should be applied when the significant wave height is larger than a given minimum wave height, HS_{min}, and the equipment cannot work at large wave heights. The leakage probability is therefore equal to 100 % at significant wave heights larger than a user specified threshold level HS_{max}. A linear reduction is applied between the minimum and maximum wave heights HS_{min} and HS_{max}. Experience has shown that the most equipment fail to work at significant wave heights larger than 4 m.

4.1.3 Effect of oil viscosity

The booms and skimmers will not work at very low oil viscosity. Likewise, the equipment is less effective at very high viscosities. A minimum viscosity of 1000 cP is mentioned by Nordvik, A.B., Daling, P. and Engelhardt, F.R. 1992. Thus a simple linear increase in the leakage probability is therefore introduced at viscosities lower than the user specified minimum oil viscosity. In the same way, a simple constant reduction in effectiveness can be introduced when the viscosity exceeds a certain maximum viscosity. According to Norsk Olje og Gass 2013 a reduction should be expected when the viscosity exceeds 10000 cP.

4.1.4 Effect of speed through water

It has long been recognized that one of the most important factors controlling the effectiveness of boom and skimmers is the speed through water (STW). A conceptual relationship between STW versa significant wave heights can be established from NOFI, 2015. Based on information on the specific equipment and safety margins the operational “window “is illustrated below. Outside the grey area the leakage probability is equal to 100 %. Model input is HS_{max}, STW_{min} and STW_{max}. At high speed through water the oil will simple spill over the boom. On the other hand, a minimum towing speed through water is also required in order to collect the oil.

4.1.5 Effect of oil slick thickness

The thinner the oil layer the more difficult it is to collect and pump the oil. For oil layer thickness larger than 0.1 mm all oil can be collected. However, the probability of “leakage” increases at lower thickness, Lewis, A. (2007) and Norsk Olje og Gass 2013. The probability of leakage due to smaller oil layer thickness is expressed using a simple regression, P = -10*layer thickness (mm) + 1.

4.1.6 Effect of Daylight vs night light

One cannot expect the same efficiency during day and night operations. After sundown a 20 % reduction in pumping capacity has been introduced. According to Norsk Olje og

Gass(2013) a 20 % reduction should be expected when the sun inclination is less than 6 deg. under the horizon.

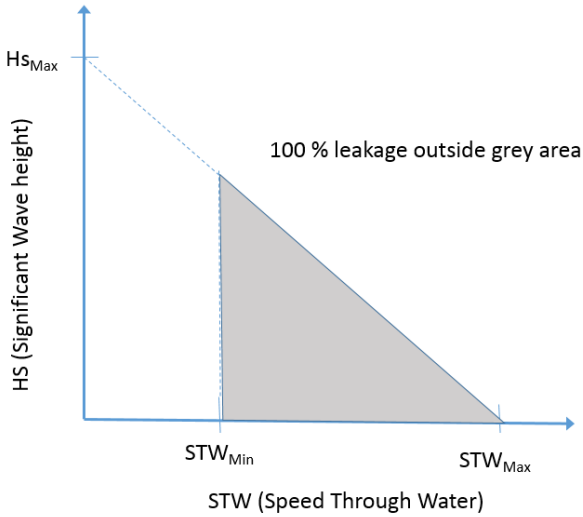

Figure 4.2 Conceptual relationship between speed through water and significant wave height

Oil may, independent of the equipment, be dispersed into the water column due to wave action and hence drift under the oil boom skirt. The depth to the skirt therefore also has to be provided as model input.

Based on the boom position, movement and the particle drift direction within a given time step the model compute whether or not an oil particle will be caught by the boom system. Once an oil particle has hit the boom it will be locked in the following time steps, independent of the movement of the boom, unless otherwise specified via the MIKE Oil Spill toolbox.

The overall probability of leakage at a given time step is then defined as the maximum of the above effect probabilities.
Internally for each time step a random number [0..1] is drawn and compared with the overall leakage probability for the oil particle in question. If the random number is smaller than the leakage probability the oil particle mass is reduced with an amount equal to the associated removal or pumping capacity. If all oil mass is removed in a given time step the particle is automatically removed from the simulation.

Please note that the probabilities work on a per time step base.

4.2 Description of the boom_file.csv format

4.2.1 Introduction

The Boom & Skimmer feature relies on the specifications of the boom segments read from an input file. The input file name is fixed to be “boom_file.csv” and the file must be present in the setup folder. This file contains the position and properties of individual boom segments. Each boom segment is defined as a straight line between a start- and end-coordinate, a pump and its capacity as well as a probability for particles slipping free once blocked by the boom. To determine if a particle movement is blocked by a boom segment, it is tested if its movement path intersects any line segment specified for the

time step. If more than one time step is defined and the current simulation time is in-between two time stamps, the positions of the last valid time step are applied. If the simulation time is larger than the last time stamp no boom will be active.

The boom input file can be generated by the graphic Boom & Skimmer tool in the Oilspill/Particle Track Toolbox. For manual editing the format is described below:

4.2.2 General format

The file is a plain text (ASCII) file. All data values must be separated by commas. All data of one record is represented in a single line, ended with a standard pair of “\r\l”. The value format is either a standard integer [integer] or a decimal [double] number.

Data layout

```
nt, maxseg, utmzon, iproj \r\l
yyyy, mm, dd, hh, min, ss, nseg, x1, y1, x2, y2, pumpID, capa,
p_release\r\l
yyyy, mm, dd, hh, min, ss, nseg, x1, y1, x2, y2, pumpID, capa,
p_release\r\l
…
```

4.2.3 Header

The first line is a header line describing the data. The first item/value describes the number of stored time steps ***nt*** in the file [integer], the second item the total maximal number of boom segment records ***maxseg*** [integer]. The third and fourth item describe the format of the spatial data used to specify the boom segment positions. The third item ***utmzon*** describe the UTM zone of the setup [integer]; the fourth item ***iproj*** is a flag [integer] that describes if the positions are given in geographic coordinates (dec. degree Latitude/Longitude, flag value “0”) or are in the same UTM projection as the setup (flag value “1”). Then ***nt*** lines with data follow.

4.2.4 Data lines

Each data line consist of a time stamp, number of boom segments and the boom segment records. The data lines must be ordered by the time stamp, the earliest definition in the 1st data line.

Time stamp

Each line starts with a time stamp consisting of 6 [integer] values representing the data record time stamp in the format **year, month, day, hour, minute, second**.

Number of boom segments

The 7th item ***nseg*** [integer] of a data line describes the number of active boom segments in the current time step (***nseg*** <= ***maxseg***). Now exactly ***nseg*** boom segment records follow.

Boom segment records

Each boom segment record consists of 7 values, describing the start coordinates (***x1, y1***), the end coordinates (***x2,y2***), the pump number (***pumpID***) [integer, valid range 1-5], the pump capacity (***capa***) [double] and the releasing probability (***p_release***) [double, valid 0-1.0 == 0-100%]. The later describes the probability of a particle being released from the boom (per time step).

4.2.5 Example

```
2, 1, 31, 1
2016,06,14,10,0,0,1,2.34, 60.01,2.34,60.11,1,0.0,0.0
2016,06,14,16,0,0,1,2.34, 60.01,2.34,60.11,1,0.0,0.0
```

This specification defines two boom time steps with at max 1 boom segment records. The setup is specified in UTM-31 coordinates and the positions inside the file are not in latitude/longitude. The first time step is the 2016/06/14 10:00:00 where the boom segment is from (2.34/60.01) to (2.34/60.11), associated with pump 1 that has a capacity of zero and the release probability is also zero. The next time step is defined at 2016/06/14 16:00:00 with the same coordinates (i.e. the boom does not move). This refers to a boom being present from 2016/06/14 10:00:00-2016/06/14 16:00:00.

5 Dispersants

Input to the modelling is the dosage of the dispersant and position of where the dispersant is applied. The dosage is then used to calculate the theoretical amount of oil that can be dispersed by the aid of dispersant.

The dispersant acts primarily by lowering the oil-water interfacial tension enabling the formation of smaller oil droplets compared to the droplets formed if no dispersant is applied. The oil-water interfacial tension of the oil treated by dispersant is set to a very low value (default value $5 \cdot 10^{-5}$ mN/m).

During a wave breaking event enabling the dispersion (see section 3.7), the amount of oil dispersed is calculated similar to the simulation of natural dispersion as described in section , and the same equation as was used in section 3.7 to calculate the droplet size distribution is used. As the dispersant lowers the oil-water interfacial tension, the oil droplets sizes are smaller than if the oil is not in contact with dispersant.

Distinction between dispersed oil with no contact with dispersant and dispersant with contact of dispersant is then made in the calculations, but the same equations for the transport and dissolution are applied for oil exposed to dispersant and oil not exposed to dispersant. As the oil droplets formed from oil exposed to dispersant are smaller than the oil droplets formed from oil not exposed to dispersant, the retention time and amount of oil dissolved in the water column is increased with the use of dispersant.

5.1 Description of the “dispergent_file.csv”

The dispersant feature relies on the specifications of the shape of the dispersant application area read from an input file. The input file name is fixed to be “dispergent_file.csv” and the file must be present in the setup folder. This file contains the position of the nodes of a closed polyline, encompassing the application area. If a particle is found to be inside the polygon, the dispersant is applied. The polygon nodes/corners should be ordered along an axis but the polygon does not need to be convex, i.e. it can be concave. However, twisted polygons should be avoided as this will lead to points inside the encompassed area may be classified as “outside”.

The dispergent input file needs to be generated manually by hand, using a plain text editor.

5.1.1 General format

The file is a plain text (ASCII) file. All data values must be separated by commas. All data of one record are represented in a single line, ended with a standard pair of “\r\l”. The value format is either a standard integer [integer] or a decimal [double] number.

Data layout

```
nt, maxcorn, utmzon, iproj \r\l
yyyy, mm, dd, hh, min, ss, ncorn, id, x1, y1, …, xncorn, yncorn \r\l
yyyy, mm, dd, hh, min, ss, ncorn, id, x1, y1, …, xncorn, yncorn \r\l
…
```

5.1.2 Header

The first line is a header line describing the data. The first item/value describes the number of stored time steps ***nt*** in the file [integer], the second item the total maximal number of polygon nodes/corners ***maxcorn*** [integer]. The third and fourth item describe the format of the spatial data used to specify the nodes/corner positions. The third item ***utmzon*** describe the UTM zone of the setup [integer]; the fourth item ***iproj*** is a flag [integer] that describes if the positions are given in geographic coordinates (dec. degree Latitude/Longitude, flag value “0”) or are in the same UTM projection as the setup (flag value “1”). Then ***nt*** lines with data follow.

5.1.3 Data lines

Each data line consist of a time stamp, number of polygon nodes/corners in the current time step, an ID and the node records. If the current time step has less than **maxcorn** nodes/corner records the remaining positions must be empty but the proper amount of data separators (coma) must be present, i.e. each data line has to have 8+(**maxcorn** * 2) items. The data lines must be ordered by the time stamp, the earliest definition in the 1st data line. Always the last valid data line is applied, i.e. the one with a time stamp <= the current simulation time. This means that a dummy time stamp with an dispergent area outside the model domain may be required if the dispergent area is not valid until the end of the simulation period.

Time stamp

Each line starts with a time stamp consisting of 6 [integer] values representing the data record time stamp in the format **year, month, day, hour, minute, second**.

Number of nodes/corners and ID

The 7th item on the data line is the number of corners/nodes in the current time step **ncorn** [integer]. The 8th item is an ID number (**id**, [integer] valid range 1-5).

Node/corner records

Now **ncorn** records of node/corner point coordinates **x,y** [double] follow. If **ncorn < maxcorn** the remaining positions must be filled with empty data.

6 In-situ Burning of Spilled Oil

In-situ burning (ISB) is a clean-up technique, which removes oil by burning it while it is still floating on the water. A minimum thickness of the oil is required for this purpose. Therefore, it is necessary to collect the oil by using specially designed fire-proof booms towed through the slick.

The DHI oil weathering model includes a description of in-situ burning. It is actually composed of different parts:

Checking of the requirements for oil to burn:

- Oil slick thickness. Generally, the minimum thickness for fresh oil to burn is two to three millimetres. For emulsified oil, the minimum thickness is probably closer to five millimetres. Oil, which is allowed to spread without restriction, will usually quickly become too thin to sustain a burn. In the DHI Oil Weathering model the default critical oil slick thickness before in-situ burning can be initiated is set at 6 mm. The user may overwrite the default critical oil slick thickness. Burning is assumed to stop, if the oil slick thickness is below 1 mm.

- Water content. If the water content is above 25% then it may not be possible to ignite the oil and that addition of an emulsion breaker may be needed. This is however not included in the DHI Oil Weather Model.

Collection of the oil

The process of collecting oil by booms in order to achieve a proper oil slick thickness for ISB is described in chapter 4. The module calculates the amount of oil within the boom and then the average oil slick thickness

Ignition

The ignition of the oil is started, when the requirement for oil to burn is fulfilled.

Burning

A burning rate of 0.06 mm/s is as default used in the calculation (see e.g. William & Roy Overstreet (1998)). The user may specify another burning rate, however many burns do not last much longer than the timestep applied in calculations, so it may not be noted if another burning rate is applied.

Stop of burning

The burning is stopped in the modelling, when the oil slick thickness has reached the minimum thickness for burning.

Output from the calculations

- *Revised composition of the oil after ISB*: It is assumed that burning is propagating so the removal of the oil fractions follows the boiling point of the oil components. This means that the oil components with the low boiling points are assumed to be burned before the oil components with higher boiling point.

- *Density of the residual*: It is a very difficult to estimate the density, as new compounds may be formed during the burning. A proper determination is however quite important, as it determines if the residual will sink or remain on the sea surface.

The approach taken is that if the calculated density exceeds the water density or if residuals of semi-volatiles are still left after the burning, then the density is calculated according to the composition of the residual oil. If this is not the case, then the user needs to specify if the oil will sink or remain on the sea surface after burning. It can be mentioned that correlations between the densities of laboratory-generated burn residues and oil properties predict that burn residues will sink in sea water when the burned oils have (a) an initial density greater than about 0.865 g/cm3 (or API gravity less than about 32°) or (b) a weight percent distillation residue (at >1000°F (~540°C)) greater than 18.6%. When these correlations are applied to 137 crude oils, 38% are predicted to sink in seawater, 20% may sink, and 42% will float (NOAA 2016).

- *Generation of soot*: The amount of generated soot is calculated from: Generated soot (kg) = Amount of burned oil (kg)·[0.11+0.03·log10(R)] (Fraser et al. 1997) where R is the radius of the oil slick (area enclosed in the booms).
- *Generation of PAHs*. Burning will remove the oil components. Some new compounds will be formed during the burning. PAHs will as the other hydrocarbons be partly removed by burning, but it has been found that some PAHs are found in higher amounts than before burning. The generation of dissolved PAH is not yet implemented.

7 Beaching, Shore Lock-Reflection Conditions

The DHI oil weathering model includes a simple beaching model.

The user can supply a spatial 2D map for the probability to lock an oil particle when it is washed on land. Once a particle gets locked on shore no further movement is allowed and only the following weathering process are included in the calculations:

- Biodegradation
- Photo-Oxidation
- Evaporation

By providing different values for the probability to get locked on shore, it is possible to represent the different shore properties. A hard bottom shore or a harbour with sheet pilings will not absorb much oil, thus the locking probability is low. On the other hand, wetlands will entrain most of the oil (thus have a high probability). The principal mechanism works the same way as described for the movement block (Section 4).

Please note that the beaching lock works on a per-beaching event base, and thus also depends on the time step. Appendix F describes the calculation of the probability numbers.

8 Oil in Ice-infested Waters

In ice-infested waters, oil may be trapped in the ice.

The following features are implemented:

- The oil may either adhere to the ice or being free to move away
- Submerged oil is free to move under the ice
- The oil will drift with the ice for ice fractions/concentrations larger than 30 %. At lower ice fractions the oil move according to current and wind
- Weathering processes are modified in case of ice cover (e.g. there is no entrainment due to wave activity)

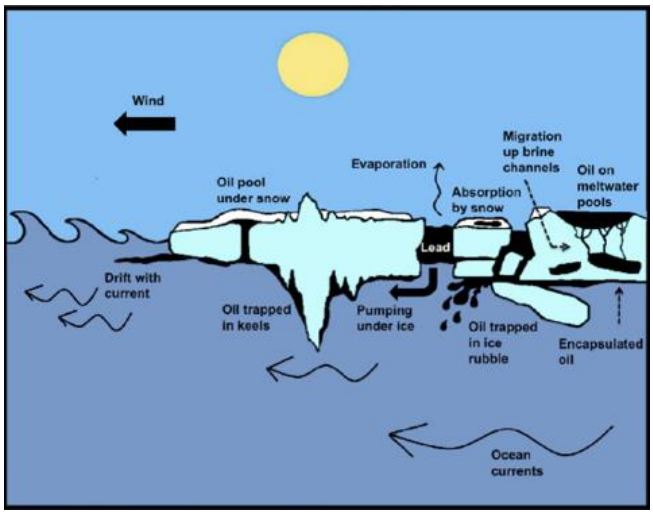

Figure 8.1 Schematic influence of sea ice on oil spills (from Drozdowski et al. 2011)

9 Drift

The combined effects of current, wind drag and bed drag cause the drift of the oil particles.

The drift vector is normally varying in space. It represents the combined effects of current and wind drag that cause the advection of the particles.

$$\vec{a}(x,y,z,t) = f\left(current, wind\ drag, bed\ drag\right) \tag{9.1}$$

The drift profile is a description of the vertical variation of the drift regime that influences the particles. It will normally be the currents and the wind that governs the shape of the drift profile. Currents and wind are already calculated in the hydrodynamic setup, but for 2D hydrodynamics it is the depth average values that are the output of the hydrodynamic setup. By assuming some shapes of the vertical drift profile it is possible to get a more realistic current profile than just a depth integrated value, and therefore a more realistic drift of particles.

9.1 Bed shear profile (logarithmic profile)

The shape of the velocity profile within a turbulent boundary layer is well established by both theory and experiment. The profile has specific characteristics very close to the bed where viscosity controls the vertical transport of momentum, and different characteristics farther from the bed where turbulence controls the vertical transport of momentum.

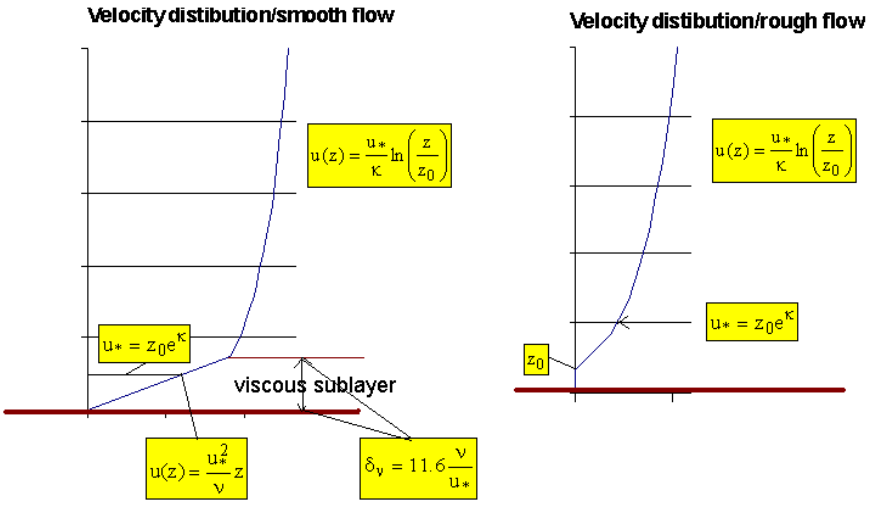

Figure 9.1 Example of bed shear profile applied from 2D flow fields

The region closest to the bed boundary is called the laminar sub-layer or viscous sub-layer, because within the region turbulence is suppressed by viscosity. The viscous, laminar sub-layer only plays a significant role for smooth flows, where a typical thickness of the viscous layer is about 2 cm, whereas for rough flows the viscous sub layer is typically less than 1 mm, and instead the flow is set to zero for z smaller than z0.

Logarithmic layer (z >= δ_v smooth flow) (z >= z0 rough flow)

$$u = \frac{2.3}{k} \cdot u^* \cdot \log_{10} \frac{z}{z_0} \tag{9.2}$$

Smooth flow: Laminar bed shear layer (z < δ_s)

$$u = \left(u^*\right)^2 \cdot \frac{z}{\nu} \tag{9.3}$$

Where:

κ	Von Karman empirical constant 0.4
z_0	Characteristic roughness
z	Coordinate from bed towards water surface [m]
u^*	Friction velocity
δ_v	Thickness of viscous bed shear layer
ν	Kinematic viscosity of water

9.2 Wind induced profile

The wind drag can also cause increased flow velocities in the upper part of the water column, and corresponding velocities in the opposite direction in the lower part. In 3D hydrodynamics this effect is included in the hydrodynamic output, but that is not the case with the depth averaged 2D hydrodynamics. So if this flow regime should be described with 2D hydrodynamics, a wind induced profile must be applied, which will distribute the depth averaged flow in the water column.

This has been done by calculating a wind drift vector that is multiplied with the current velocity vector.

The magnitude of the surface wind drift vector c_w^* is commonly assumed to be proportional to the magnitude of the wind speed 10 m above the sea surface. This factor c_w^* has a common value that varies from 3 to 4 per cent of the wind speed 10 m above the sea surface (from Al-Rabeh (1994)).

The vertical distribution of the wind drift vector consists of an offshore part and an onshore part. The onshore distribution is based on a parabolic vertical profile and is able to produce backflow at depths, where the offshore logarithmic profile does not.

The parabolic profile acts in shallow waters with a water depth less than a specified water depth, hsep, which is a positive value (in metres) and measured from the free water surface.

The vertical distribution of the parabolic onshore profile is given by:

$$c_w(z) = c_w^* \left(1 - 3\frac{z}{h}\right)\left(1 - \frac{z}{h}\right) \tag{9.4}$$

Where:

h	Local water depth in meter
z	Vertical particle co-ordinate, measured from sea surface
c_w^*	Wind drift factor (input)

The parabolic profile causes the wind-generated flow in the upper third of the water column to be in the same direction as the current and the flow in the lower part to be in the opposite direction of the wind. There is no net depth averaged mass transport due to the wind.

The vertical distribution of the offshore wind drift vector is given by:

$$c_w(z) = c_w^* \exp\left(-k_0\, z\right) \tag{9.5}$$

Where:

k_0	3/hw [m-1]
h_w	Depth of wind influence [m]
z	Vertical co-ordinate measured from sea surface
c_w^*	Wind drift factor [-]

9.3 Wind Acceleration of Surface Particles

Particles that are exposed to wind in the water surface are affected according to the wind regime in 2 ways: indirectly via the currents that include the wind, but also directly as an extra force directly on the particle. How much of the wind speed that is transferred to the particle speed depends on the nature of the particle: how much is the particle exposed, etc. Therefore, it is a calibration factor that expresses how much of the wind speed that is added to the particle speed.

In the Particle Tracking Module the wind acceleration of surface particles affect the drift with the following modification:

When the particle is in the top 5 cm of water column:

$$U_{particle} = U_{current} + windweigth \cdot W \cdot \sin\left(Winddirection - \pi + \theta_w\right) \tag{9.6}$$

$$V_{particle} = V_{current} + windweigth \cdot W \cdot \cos\left(Winddirection - \pi + \theta_w\right) \tag{9.7}$$

Where:

θ_w	Wind drift angle
windweight	Calibration factor for wind drag on particle

Please note that the wind drift angle is related to the geographic location, see next section.

9.3.1 Wind drift angle

The Coriolis force is normally included in the hydrodynamic currents, but also for the wind acceleration of surface particles the Coriolis force must be considered.

Due to the influence from the Coriolis force, the direction of the wind drift vector is turned relatively to the wind direction. The angle θw of deviation is termed with the wind drift angle. It turns to the right (positive) on the Northern Hemisphere and to the left (negative) on the Southern Hemisphere. The magnitude of the wind drift angle varies with the geographical location and wind speed and it is often estimated at 12-15 degrees in the North Sea. Samuels et al 1985 and Al-Rabeh (1994) give a wind speed dependent drift angle as

$$\theta_w = \beta \exp\left(\frac{\alpha |U_w|^3}{g\gamma_w}\right) \tag{9.8}$$

Where:

	Al-Rabeh(2004)	Samuels et al. (1985)
α	$-0.31*10^{-8}$	-10^{-8}
β	28°28' (28.6333)	25° (25.0)

γ_w Kinematic viscosity [m²/s]
g Acceleration due to gravity [m/s2]

10 References

/1/ Al-Rabeh, A., 1994. Estimating surface oil spill transport due to wind in the Arabian Gulf. Ocean Engineering 21:461-465. doi: 10.1016/0029-8018(94)90019-1.

/2/ Betancourt F., A. Palacio, and A. Rodriguez, 2005. Effects of the Mass Transfer Process in Oil Spill. American Journal of Applied Science 2:939-946.

/3/ Delvigne, G., and C. Sweeney, 1988. Natural dispersion of oil. Oil and Chemical Pollution 4:281-310. doi: 10.1016/S0269-8579(88)80003-0.

/4/ Drozdowski A., S. Nudds, C. G. Hannah, H. Niu, I. Peterson and W. Perrie (2011): Review of Oil Spill Trajectory Modelling in the Presence of Ice. Canadian Technical Report of Hydrographic and Ocean Sciences 274. 2011

/5/ Fate of Marine Oil Spills, 2002. Page 8. Technical Reports, The International Tanker Owners Pollution Federation Limited (ITOPF), London.

/6/ Fingas, M. F., 1996. The evaporation of oil spills: Prediction of equations using distillation data. Spill Science & Technology Bulletin 3:191-192. doi: 10.1016/S1353-2561(97)00009-1.

/7/ Fingas, M. F., 1997. Studies on the evaporation of crude oil and petroleum products: I. the relationship between evaporation rate and time. Journal of Hazardous Materials 56:227-236. doi: 10.1016/S0304-3894(97)00050-2.

/8/ Fingas, M.F., 2004. Modeling evaporation using models that are not boundary-layer regulated. Journal of Hazardous Materials, Volume 107, 2004, pp. 27-36.

/9/ French-McCay, D. P.,2004. Oil spill impact modeling: Development and validation. Environmental Toxicology and Chemistry 23:2441-2456. doi: 10.1897/03-382.

/10/ Johansen, Brandvik, and Farooq (2013), “Droplet breakup in subsea oil releases - Part 2. Predictions of droplet size distributions with and without injection of chemical dispersants.”. Marine Pollution Bulletin, 73:327-335. doi:10.1016/j.marpolbul.2013.04.012.

/11/ Jirka, G.H (2004). “Integral Model for Turbulent Buoyant Jets in Unbounded Stratified Flows. Part 1: The Single Round Jet”, end. Fluid Mech., Vol. 4 , 1-56

/12/ The International Tanker Owners Pollution Federation Limited (ITOPF) (2002): Fate of Marine Oil Spills. Technical Information Paper. http://www.cleancaribbean.org/download_pdf.cfm?cF=ITOPF%20Technical%20Information%20Papers%20(TIPS)&fN=Fate-of-Marine-Oil-Spills.pdf

/13/ Lee, J.H.W., Cheung, V., Wang, W.P. and Cheung, S.K.B. (2000). " Lagrangian modeling and visualization ofrosette outfall plumes", Proceedings of the Hydroinformatics 2000, University of Iowa, Jul. 2000.

/14/ JETLAG2008 -An Update. Available from: https://www.researchgate.net/publication/266877032_JETLAG2008_-An_Update [accessed Jan 11, 2017].

/15/ Lehr, W.J., 2001. Review of modeling procedures for oil spill weathering behaviour

/16/ Li Zheng, Poojitha D. Yapa , 2000 “Buoyant Velocity of Spherical and Nonspherical Bubbles/Droplets”, Journal of Hydraulic Engineering, November 2000, Volume 126, issue 1

/17/ Mackay, D., I. Buist, R. Mascarenhas, and S. Paterson, 1980. Oil spill processes and models. Environmental Emergency Branch, Department of Fisheries and Environment, Environment Canada, Ottawa, ON.

/18/ Mackay, D., and W. Zagorski, 1982. Water-in-oil emulsions: a stability hypothesis. Proceedings of the Fifth Annual Arctic Marine Oilspill Program Technical Seminar:61-74.

/19/ Reed, M., 1989. The physical fates component of the natural resource damage assessment model system. Oil and Chemical Pollution 5:99-123. doi: 10.1016/S0269-8579(89)80009-7.

/20/ Sebastião, P., and C. Guedes Soares, 1995. Modeling the fate of oil spills at sea. Spill Science & Technology Bulletin 2:121-131. doi: 10.1016/S1353-2561(96)00009-6.

/21/ Xie, H., P. D. Yapa, and K. Nakata, 2007. Modeling emulsification after an oil spill in the sea. Journal of Marine Systems 68:489-506. doi: 10.1016/j.jmarsys.2007.02.016.

/22/ Johansen, Ø., “DeepBlow – A Lagrangian Plume Model for Deep Water Blowouts”, Spill Science & Technology Bulletin , 2:103-111, 2000.

/23/ Norsk Olje og Gass (2013). Veiledning for miljørettede beredskapsanalyser. Oslo, Norway, Norsk Olje og Gass: 1-31.

/24/ Nordvik, A. B. (1999). "Summary of development and field testing of the transrec oil recovery system." Spill Science & Technology Bulletin 5(5/6): 309-322.

/25/ Nordvik, A.B., Daling, P. and Engelhardt, F.R. 1992. Problems in the interpretation of spill response technology studies. In: Proceedings of the 15th AMOP Tecnical Seminar, June 10-12, Edmonton, Alberta, Canada, pp. 211-217.

/26/ Lewis, A. (2007). Current Status of the BAOAC (Bonn Agreement Oil Appearance Code): 19.

/27/ NOFI, 2015 (unpublished)

/28/ William J. Lehr & Roy Overstreet (1998): Smoke plume screening tool for in-situ burning. Transactions on Ecology and the Environment, Vol. 20, © 1998 WIT Press, www.witpress.com, ISSN 1743-3541

/29/ Fraser, J., I. Buist, and J. Mullin, 1997. A Review of the Literature on Soot Production During In-situ Burning of Oil. Proceedings of the Twentieth Arctic and Marine Oil Spill Program (AMOP) Technical Seminar, Environment Canada, Ottawa, Canada, pp. 669-683.

/30/ Johansen Øistein, Mark Reed, Nils Rune Bodsberg (2015): Natural dispersion revisited. Marine Pollution Bulletin 93 (2015) 20–26

/31/ NOAA (2016): Residues from In Situ Burning of Oil on Water. http://response.restoration.noaa.gov/oil-and-chemical-spills/oil-spills/resources/residues-in-situ-burning-oil-water.html

/32/ Samuels W.B., Huang N.E., Amsiuiz, D.E. (1985): An Oilspill Trajectory Analysis Model with a Variable Wind Deflection Angle. Ocean Energy, Vol.9, No.4 pp. 347-360

/33/ Yapa, P.D., and Zheng, L., (1997). "Simulation of Oil Spills from Underwater Accidents I: Model Development," Journal of Hydraulic Research, IAHR, October, 673-688

/34/ Yapa Poojitha D. & Zheng Li (1997): Simulation of oil spills from underwater accidents I: model development. Journal of Hydraulic Research, 35(5), 673-688.

/35/ Yapa, P.D. (2010). "Coastal Pollution due to Oil Spills," in H. J. S. Fernando (ed) , Handbook of Environmental Fluid Dynamics, Taylor & Francis Books Inc., (in progress).

/36/ Yapa, P. D, Dasanayaka, L. K., Bandara, U. C., and Nakata, K. (2010). "A Model to Simulate the Transport and Fate of Gas and Hydrates Released in Deepwater, Journal of Hydraulic Research, IAHR. (accepted for publication)

/37/ Dasanayaka, L. K., and Yapa, P. D. (2009). "Role of Plume Dynamics on the Fate of Oil and Gas Released Underwater," Journal of Hydro-Environment Research, IAHR/Elsevier, March, 243-253

/38/ Nakata, K., Yapa, P. D, Dasanayaka, L. K., Bandara, U. C., and Suzuki, S. (2008). "Shinkaiiki kara rouhi ni shite methan gasu kyodou soku modaruno kaihatsu -in Japanese (English translation : A Model for Methane gas in Deepwater)," Aquabiology, Seibutsu Kenkyusha, Tokyo, Japan, August, Vol. 30., No. 4.

/39/ Xie, H., Yapa, P. D., and Nakata, K. (2007) "Modeling Emulsification after an Oil Spill in the Sea," Journal of Marine Systems, Elsevier, 68 (2007), 489-506.

/40/ Chen, F.H. and Yapa, P. D., (2007). "Estimating the Oil Droplet Size Distributions in Deepwater Oil Spills," Journal of Hydraulic Engineering, ASCE, February, Vol. 133. No. 2, 197-207

/41/ Xie, H. and Yapa, P. D. (2006) "Developing A Web-Based System For Large Scale Environmental Hydraulics Problems With An Application To Oil Spill Modeling, , Journal of Computing in Civil Engineering, ASCE, May, Vol. 20 (3), 197-209.

/42/ Chen, F.H, Yapa, P. D., and Nakata, K. (2004). "Simulating the Biological Effect of Oil Spills in Tokyo Bay by Using A Coupled Oil Spill - Toxicity Model," Journal of Advanced Marine Science Technology, AMTEC, Tokyo, Japan, 9(2), 131-155.

/43/ Xie, H. and Yapa, P.D. (2003). "Simulating the Behaviour and the Environmental Effect of Sediment Plumes from Deepwater Mining," Journal of Advanced Marine Science Technology, AMTEC, Tokyo, Japan, 9(1), 7-35.

/44/ Chen, F.H. and Yapa, P.D. (2004). "Modeling Gas Separation From a Bent Deepwater Oil and Gas Jet/Plume," Journal of Marine Systems, Elsevier, the Netherlands, Vol. 45 (3-4), 189-203

/45/ Zheng, L., Yapa, P. D., and Chen, F.H. (2003). "A Model for Simulating Deepwater Oil and Gas Blowouts - Part I: Theory and Model Formulation" Journal of Hydraulic Research, IAHR, August, 41(4), 339-351

/46/ Chen, F.H. and Yapa, P.D. (2003). "A Model for Simulating Deepwater Oil and Gas Blowouts - Part II : Comparison of Numerical Simulations with "Deepspill" Field Experiments", Journal of Hydraulic Research, IAHR, August, 41(4), 353-365

/47/ Zheng, L. and Yapa, P.D. (2002). "Modeling Gas Dissolution in Deepwater Oil/Gas Spills," Journal of Marine Systems, Elsevier, the Netherlands, March, 299-309

/48/ Yapa, P. D., Zheng, L, and Chen, F.H. (2001). "A Model for Deepwater Oil/Gas Blowouts," Marine Pollution Bulletin, The International Journal for Marine Environmental Scientists/Engineers, Elsevier Science Publications, UK, Vol. 43, No. 7, 234-241.

/49/ Chen, F.H. and Yapa, P.D. (2001). "Estimating Hydrate Formation and Decomposition of Gases Released in a Deepwater Ocean Plume," Journal of Marine Systems, Elsevier, the Netherlands, Vol. 30/1-2, 21-32

/50/ Zheng, L. and Yapa, P.D. (2000). "Buoyant Velocity of Spherical and Non-Spherical Bubbles/ Droplets," Journal of Hydraulic Engineering, ASCE, November, 852-855

/51/ Yapa, P.D., Zheng, L., and Nakata, K. (1999). "Modeling Underwater Oil/Gas Jets and Plumes," Journal of Hydraulic Engineering, ASCE, May, 481-491

/52/ Yapa, P.D., and Weerasuriya, S.A., (1997). "Spreading of Oil Spilled under Floating Broken Ice," Journal of Hydraulic Engineering, ASCE, August, 676-683.

/53/ Yapa, P.D. (editor and contributor), (1996). "State-of-the-Art Review of Modeling Transport and Fate of Oil Spills," by the ASCE Task Committee on Modeling of Oil Spills, Journal of Hydraulic Engineering, ASCE, Double Length Paper, November, 594-609.

/54/ Yapa, P.D., Zheng, L., and Kobayashi, T., (1996). "Application of Linked-List Approach to Pollutant Transport Models," Journal of Computing in Civil Engineering, ASCE, Vol. 10 (1), January 88-90.

/55/ Yapa, P.D., (1994). "Oil Spill Processes and Model Development," Journal of Advanced Marine Technology, AMTEC, Tokyo, Japan, March, 1-22.

APPENDICES

APPENDIX A

Parameterization of Oil

A Parameterization of Oil

Each crude oil type has a different composition of the various components and it may be difficult to obtain the characteristics for the composition used in the DHI oil weathering model. If available, the distillation data will provide valuable information.

As an example on how to derive input parameters for an oil spill model, the oil type 'STATFJORD' from the Norwegian North Sea is used. You can find a data sheet on this oil type at the 'Oil Properties Database' of the Environmental Technology Center Canada[1], which includes the characterisation of many oils and refined products (464). Another possibility is to consult the ADIOS program, which includes the characterisation of more oils. Data on oils may also be retrieved from Statoils crude oil assays[2].

The information from a data sheet from the 'Oil Properties Database' of the Environmental Technology Center[3] is exemplarily used to find a parameterisation for the DHI oil weathering model.

A.1 Evaporation – simple expression

The data sheet lists the following equation for predicting the evaporation when using the simple expression for the evaporation:

$$\%\mathrm{Ev} = (2.67 + 0.06 * \mathrm{T}) * \ln(\mathrm{t}) \qquad \text{(A. 1)}$$

Where:

%Ev	the weight percent evaporated
T	the surface temperature [°C]
t	the time in minutes [min]

These data can be directly used for the model constant when using a simple evaporation formulation. Obviously this is a logarithmic evaporation type, thus the constant 'Simple Evaporation, select logarithmic or quadratic type' has to be set to '0' and the constants 'Simple Evaporation: 1st oil specific constant'=2.67 and 'Simple Evaporation: 2nd oil specific constant for temperature dependency'=0.06. In appendix E you can find a list of further common oil types and values for the simple evaporation parameterisation.

Table 10.1 Input Lagrange constants for evaporation in oil spill model setup

Description		Value
Simple Evaporation:	1st oil specific constant	2.67
Simple Evaporation:	2nd oil specific constant for temperature dependency	0.06.
Simple Evaporation, select logarithmic or quadratic type		0

[1] Environmental Technology Center Canada, http://www.etc-cte.ec.gc.ca/databases/spills_e.html

[2] http://www.statoil.com/en/OurOperations/TradingProducts/CrudeOil/Crudeoilassays/Pages/default.aspx

[3] http://www.etc-cte.ec.gc.ca/databases/OilProperties/pdf/WEB_Statfjord.pdf

The distillation data from the data sheet can be used to parameterise the general for of simple evaporation equation (taking the percent loss at 180°C, in this case 26% as shown in Figure A. 1. However, luckily the specific constants are given explicitly in the data sheet and can be entered directly into the model, see Figure A. 1.

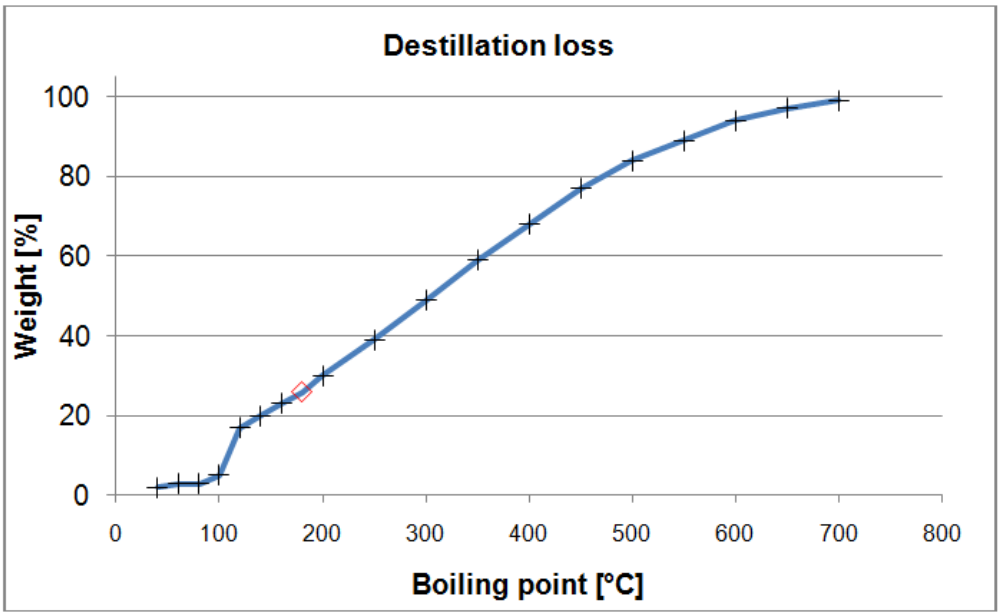

Figure A. 1 Distillation loss for oil type 'STATFJORD', marked point evaporation loss at 180°C

Table A. 1 Input Lagrange constant for evaporation

Description	Value
Simple evaporation, distillation percentage at 180ºC	26%

A.2 Distribution into Different Model Components

It is often difficult to find good estimates how the oil can be represented by the oil fractions defined in the weathering model. The distillation data can provide good information for this task. The different oil fractions of the template are defined by the molecular mass and boiling points. Note that due to the chemical structures of hydrocarbons these properties are well correlated. An Excel file has been prepared to aid the parameterisation of an oil. This excel-file is used for illustration.

1. Initial settings
   - Identification of the oil
   - Specification of the methodology for interpolation/extrapolation of oil data (linear (recommended) or quadratic)
   - Ambient temperature (°C)

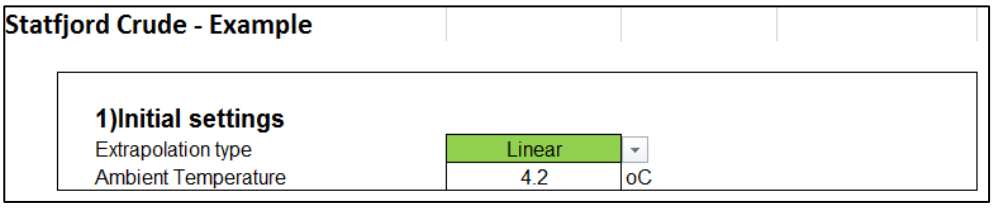

2. Overall oil properties
   - Oil density (data from data sheet)
   - Oil viscosity (data from data sheet)
   - A: Temperature coefficient for oil viscosity (viscosity(T)=viscosity(T0)*exp(-A(T-T0)). A found from data in data sheet (red value is intrapolated value):

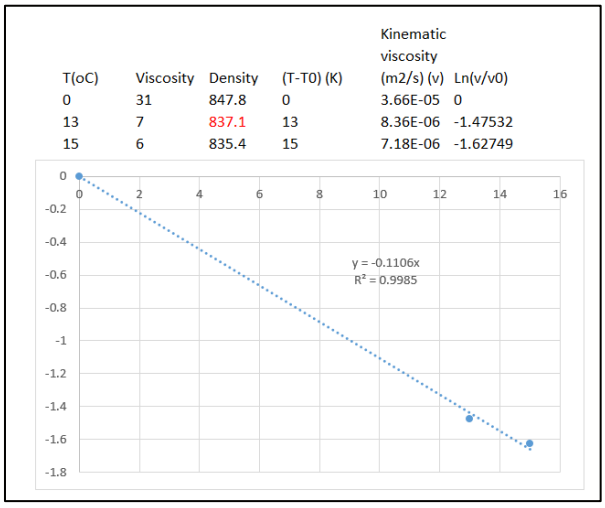

   - Pour point (data from data sheet)
   - Content of asphaltenes (data from data sheet)
   - Content of wax (data from data sheet)
   - Oil-water interfacial tension (data from data sheet)
   - Oil water interfacial tension if exposed to dispersant (default 0.001)
   - Max water content (emulsification): sometimes this data is available. For the Statfjord Crude, no data was available for this parameter. Here the max water content is calculated from:[Max water content] = =0.1074*(4.3·(1-As-Wx)^2+200*Wx^2)+0.3572, where As is the content of asphaltenes, and Wx is the

content of wax. This correlation was established on the basis of data in the ADIOS database

2)Overall oil properties

Name of oil: Statfjord Crude

	Value	Temp. (K)	Temperature coeff.
Density (kg/m3)	834.4	288.15	
Dynamic viscosity (cP)	6.0	288.15	0.11
Kinematic viscosity (m2/s)	7.19E-06	288.7	
Pour point (oC)	-3		
Asphaltenes (kg/kg (default 0.04))	0.02		
Wax (kg/kg (default 0.07))	0.08		
Oil water interfacial tension (N/m (default	0.0232		
Oil water interfacial tension (with dispersant) (N/m (default 0.001))	0.001		
Max water content (emulsification)	0.869		

3. Density, pour point and viscosity
   - Viscosity as a function of the degree of evaporation (from data sheet)
   - Pour point (PP) as a function of the degree of evaporation (from data sheet)
   - Density as a function of the degree of evaporation (from data sheet)

Note that the data sheet for the oil only gives information on the degree of evaporation on a weight basis, and not a volume basis. The degree of evaporation on a volume basis is calculated from

Evap(%volume)= 100-{100-EVAP(%weight))/Dens(%Weight)}/(1/Dens(0))

$$\%\mathrm{Evap(vol)} = 100 - \frac{100 - \frac{\%Evap(weight)}{Dens(\%Weight)}}{\frac{1}{Dens(0)}} \qquad \text{(A. 2)}$$

Where
Dens(%Weight) is the density of the remaining oil after %Weight has evaporated

3)Density, pour point and viscosity — After having entered the data click "Ctrl+Shift+w"

Temp. (K)	Evap (vol%)	PP (oC)	Viscosity (m2 s)	Density	Evap (wt%)
280	0.0	-3	7.19E-06	835.40	0.0
397.0	15.9	3	1.97E-05	864.20	13.0
455.5	26.7	17	5.35E-05	877.80	23.0
534.0	41.2	24	2.69E-04	895.70	37.0

Correlations of the degree of evaporation (volume based) with density, PP and viscosity is then automatically established – see below. Note e.g. that the $A_{viscosity}$, $B_{viscosity}$, $C_{viscosity}$ (section 3.11.1) are read from here.

		A	B	C	0	100
Density	Linear		1.452285	837.8279	838	983
	Quadratic	-0.01135	1.917884	835.6342	836	914
PP	Linear		0.775434	-3.90167	-3.9	73.6
	Quadratic	4.34E-05	0.773821	-3.89467	-3.9	73.9
Viscosity	Linear		0.098222	-11.9762	6.29E-06	1.16E-01
	Quadratic	0.000803	0.068392	-11.8468	7.16E-06	2.05E+01
TEMP	Linear		6.122886	288.2636	288	901
	Quadratic	-0.03828	7.693621	280.8631	281	667

4. Distillation curve

In this part the distillation curve for the oil is entered. Both the volume fraction evaporated and the weight fraction evaporated as a function of temperature is entered. Note that for the actual oil, the data sheet only gives information on the weight basis, and the degree of evaporation on volume basis is calculated on the basis of the above equation.

4)Destillation curve After having entered the destillation curve click "Ctrl+Shift+U"

Boiling point (K)	Fraction (L/L)	Fraction (kg/kg)	Density
311	0	0.000	835.4
313	0.028	0.020	842.2
333	0.040	0.030	843.8
353	0.040	0.030	843.8
373	0.063	0.050	847.0
393	0.200	0.170	866.3
413	0.233	0.200	871.1
433	0.266	0.230	875.9
453	0.298	0.260	880.7
473	0.341	0.300	887.2
523	0.435	0.390	901.6
573	0.536	0.490	917.7
623	0.633	0.590	933.8
673	0.718	0.680	948.2
723	0.800	0.770	962.7
773	0.863	0.840	973.9
823	0.906	0.89	982.0
873	0.949	0.94	990.0
923	0.975	0.97	994.8
973	0.992	0.99	998.1

Correlations for the prediction of the degree of evaporation as a function of temperature are then automatically established – see below.

		Coefficients A	B	C	Fraction evaporated (-) 0	1
Weight	Linear	0.001646203	-0.490628093		298	905
	Quadratic	-1.13923E-06	0.003059319	-0.874524002	325	946
Volume	Linear	0.00163721	-0.461821784		282	893
	Quadratic	-1.53207E-06	0.00353761	-0.978096343	321	950

5. Define oil fraction

- The upper temperature for the VOLATILE and the SEMI-VOLATILE fractions defines the three oil fraction. Generally, it is attempted to make the fraction of similar sizes

5)Define oil fractions

Define oil fractions	Upper boiling point (K)	Volume fraction	Weight fraction
Light	450	0.3036	0.27
Medium*	650	0.3705	0.36
Heavy	>650	0.3259	0.37
*Default value:	530		

The below figure is always shown in the excel file. It shows the distillation curves and the cut-of temperatures defining the three oil fractions.

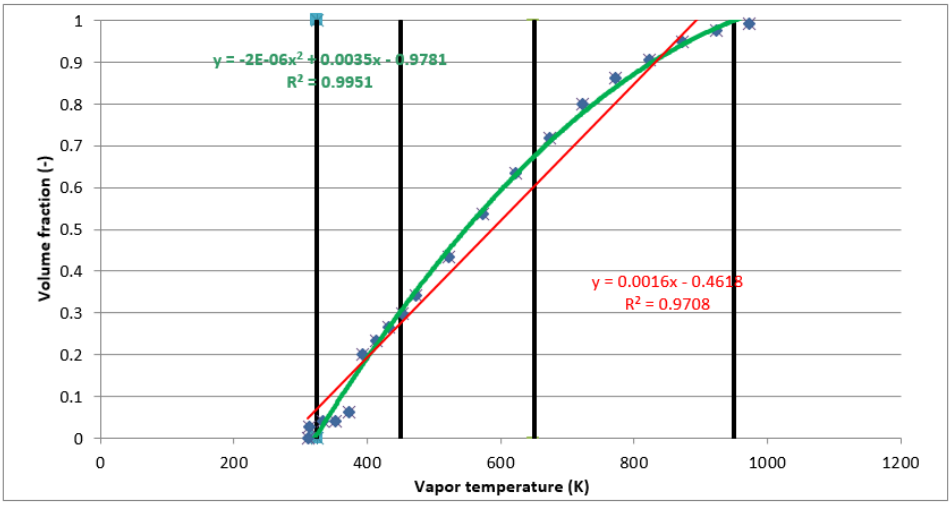

6. Characterisation of the oil fractions
Several parameters are needed to characterise each fraction. Calculated or default values are automatically inserted. Notice that default values (biodegradation rate, photooxidation rate, dissolution rate constant, volume expansion coefficient) can be overwritten. As the density is often specified at different temperatures, it straight-forward to calculate the volume expansion coefficient.

6)Characterisation of oil fractions After having entered all data click Ctrl+Shift+y

		Light	Medium	Heavy (light end)
Parameter	Unit	I	II	III (lower)
Weight fraction		0.27	0.36	0.37
Volume fraction		0.30	0.37	0.33
BP-lower	K	325	450	650
BP-higher	K	450	650	950
Viscosity	m2 s	2.4E-05	1.1E-03	5.3E-01
Density	kg/m3	693	883	913
Volume expan. Coef.	1/deg C	0.0007	0.0007	0.0007
MW	g/mole	153	333	519
PP (oC)	oC	-50	20	48
CwSat (min)	kg/kg	2.83E-07	4.88E-08	5.61E-09
CwSat (max)	kg/kg	1.59E-03	3.49E-07	4.83E-07
CwSat (avg)	kg/kg	1.18E-04	1.56E-07	7.17E-08
Psat (atm) at (oC):	0	4.9E-03	8.2E-07	8.2E-07
Psat (atm) at (oC):	5	6.4E-03	1.5E-06	1.5E-06
Psat (atm) at (oC):	10	8.4E-03	2.6E-06	2.6E-06
Psat (atm) at (oC):	4.2	6.2E-03	1.4E-06	1.4E-06
Psat-min at (oC)	4.2	6.2E-03	1.4E-06	8.9E-17
Psat-max at (oC)	4.2	2.8E-01	6.2E-03	1.4E-06
C21		6.8E+01	1.1E+02	1.1E+02
DelSa		1.4E+01	1.4E+01	1.4E+01
DelZb		9.7E-01	9.7E-01	9.7E-01
Dissolution rate	1/day	0.4000	0.4000	0.4000
Biodegration decay	1/day	0.0050	0.0010	0.0000
Photooxidation deca	1/day	0.0000	0.0000	0.0000
Sw		1.2E-04	1.6E-07	7.2E-08

APPENDIX B

Evaporation Parameters for Different Oils

B Evaporation Parameters for Different Oils

The time-dependent correlations for evaporation loss as suggested by Fingas (1996) and (1997) are also included in the DHI oil spill model. Based on empirical studies on the evaporation of oil and petroleum products, Fingas determined best-fit equations for both the percentage loss by time and absolute weight loss for various oil types. Most oils were found to follow logarithmic loss curves, but a smaller amount fitted square root loss curves with time for periods up to about 5 days. The derived relationships are of the general structure:

Evaporation curve type: logarithmic form

$$\text{loss}\ (\%\text{weight}) = (\mathrm{A} + \mathrm{B} \cdot \mathrm{T}) \cdot \ln(\mathrm{t}) \tag{B. 1}$$

Evaporation curve type: square root form

$$\text{loss}\ (\%\text{weight}) = (\mathrm{A} + \mathrm{B} \cdot \mathrm{T}) \cdot \sqrt{\mathrm{t}} \tag{B. 2}$$

Where:

A	Oil specific constant (called evapA in the DHI model)
B	Oil specific constant for temperature dependency (called evapB in the DHI model)
T	Oil temperature [°C]
t	Age of the oil [minutes]

The oil specific constants A and B as well as the type of the evaporation curve are often available for specific oils and can be found in literature. A list for common oils can be found in below table.

The oil temperature is assumed to be equal to the ambient water temperature.

The loss equation constants were found to correlate fine with the percentage distilled at 180°C (r^2 between 0.74 and 0.98, Fingas (1996). If the specific values for A and B are not known, the distillation loss at 180°C can be used instead. The model allows specifying this distillation loss at 180°C directly. In this case some generic forms for the evaporation loss equations are used:

Evaporation curve type: logarithmic, generic form

$$\text{loss}\ (\%\text{weight}) = (0.165 \cdot \mathrm{D} + 0.045 \cdot (\mathrm{T} - 15)) \cdot \ln(\mathrm{t}) \tag{B. 3}$$

Evaporation curve type: square root form

$$\text{Loss}\ (\%\text{weight}) = \left(0.0254 \cdot \mathrm{D} + 0.01 \cdot (\mathrm{T} - 15)\right) \cdot \sqrt{\mathrm{t}} \tag{B. 4}$$

Where:

D	distillation loss (weight %) at 180°C (called evap180 in the DHI model)
T	Oil temperature [°C]
t	Age of the oil spill [minutes]

Please note that a value (> 0%) for the constant D (distillation loss at 180°C) in the model parameterisation will override any specific values A and B. There are possible temperature constrains when applying the simplified evaporation scheme; the generic forms should not be used below a temperature of 15°C

Oil-type	Curve type	A	B	T [°C] >
Adgo	1	0.11	0.013	---
Adgo-long term	0	0.68	0.045	---
Alberta Sweet Mixed Blend	0	3.24	0.054	---
Amauligak	0	1.63	0.045	---
Amauligak-f24	0	1.91	0.045	---
Arabian Heavy	0	1.31	0.045	---
Arabian Heavy	0	2.71	0.045	---
Arabian Light	0	2.52	0.037	---
Arabian Light	0	3.41	0.045	---
Arabian Light (2001)	0	2.4	0.045	---
Arabian Medium	0	1.89	0.045	---
ASMB - Standard #5	0	3.35	0.045	---
ASMB (offshore)	0	2.2	0.045	---
Av Gas 80	0	15.4	0.045	---
Avalon	0	1.41	0.045	---
Avalon J-34	0	1.58	0.045	---
Barrow Island	0	4.67	0.045	---
BCF-24	0	1.08	0.045	---
Belridge Cruide	1	0.03	0.013	---
Bent Horn A-02	0	3.19	0.045	---
Beta	1	-0.08	0.013	6
Beta - long term	0	0.29	0.045	---
Boscan	1	-0.15	0.013	12
Brent	0	3.39	0.048	---
Bunker C Anchorage	1	-0.13	0.013	10
Bunker C Anchorage - long term	0	0.31	0.045	---
Bunker C -long term	0	-0.21	0.045	5
Bunker C -short term	1	0.35	0.013	---
Bunker C-Light (IFO-250)	1	0.0035	0.0026	---
California API 11	1	-0.13	0.013	10
California API 15	1	-0.14	0.013	11
Cano Limon	0	1.71	0.045	---
Carpenteria	0	1.68	0.045	---
Cat cracking feed	1	-0.18	0.013	14
Chavyo	0	3.52	0.045	---
Combined Oil/gas	1	-0.08	0.013	6
Compressor Lube Oil (new)	0	-0.68	0.045	15
Cook Inlet - Swanson River	0	3.58	0.045	---
Cook Inlet - Granite Point	0	4.54	0.045	---
Cook Inlet Trading Bay	0	3.15	0.045	---
Corrosion Inhibitor Solvent	1	-0.02	0.013	2
Cusiana	0	3.39	0.045	---

Oil-type	Curve type	A	B	T [°C] >
Delta West Block 97	0	6.57	0.045	---
Diesel - long term	0	5.8	0.045	---
Diesel Anchorage - Long	0	4.54	0.045	---
Diesel Anchorage - Short	1	0.51	0.013	---
Diesel Fuel - southern - long term	0	2.18	0.045	---
Diesel Fuel - southern - short term	1	-0.02	0.013	2
Diesel Mobil 1997	1	0.03	0.013	---
Diesel Mobil 1997 - long term	1	-0.02	0.013	2
Diesel Regular stock	1	0.31	0.018	---
Dos Cuadros	0	1.88	0.045	---
Edicott	0	0.9	0.045	---
Ekofisk	0	4.92	0.045	---
Empire Crude	0	2.21	0.045	---
Esso Spartan EP-680 Industrial Oil	0	-0.66	0.045	15
Eugene Island 224 - condensate	0	9.53	0.045	---
Eugene Island Block 32	0	0.77	0.045	---
Eugene Island Block 43	0	1.57	0.045	---
Evendell	0	3.38	0.045	---
FCC Heavy Cycle	1	0.17	0.013	---
FCC Light	1	-0.17	0.013	13
FCC Medium Cycle	1	-0.16	0.013	12

Oil-type	Curve type	A	B	T [°C] >
FCC-VGO	1	2.5	0.013	---
Federated	0	3.47	0.045	---
Federated (new-1999)	0	3.45	0.045	---
Garden Banks 387	0	1.84	0.045	---
Garden Banks 426	0	3.44	0.045	---
Gasoline	0	13.2	0.21	---
Genesis	0	2.12	0.045	---
Green Canyon Block 109	0	1.58	0.045	---
Green Canyon Block 184	0	3.55	0.045	---
Green Canyon Block 65	0	1.56	0.045	---
Greenplus Hydraulic Oil	0	-0.68	0.045	15
Gullfaks	0	2.29	0.034	---
Heavy Reformate	1	-0.17	0.013	13
Hebron MD-4	0	1.01	0.045	---
Heidrun	0	1.95	0.045	---
Hibernia	0	2.18	0.045	---
High Viscosity Fuel Oil	1	-0.12	0.013	9
Hondo	0	1.49	0.045	---
Hout	0	2.29	0.045	---
IFO-180	1	-0.12	0.013	9
IFO-30 (Svalbard)	0	-0.04	0.045	1
IFO-300 (old Bunker C)	1	-0.15	0.013	12
Iranian Heavy	0	2.27	0.045	---
Issungnak	0	1.56	0.045	---

Oil-type	Curve type	A	B	T [°C] >
Isthmus	0	2.48	0.045	---
Jet 40 Fuel	0	8.96	0.045	---
Jet A1	1	0.59	0.013	---
Jet Fuel (Anch)	0	7.19	0.045	---
Jet Fuel (Anch) short term	1	1.06	0.013	---
Komineft	0	2.73	0.045	---
Lago	0	1.13	0.045	---
Lago Tecco	0	1.12	0.045	---
Lucula	0	2.17	0.045	---
Main Pass Block 306	0	2.28	0.045	---
Main Pass Block 37	0	3.04	0.045	---
Malongo	0	1.67	0.045	---
Marinus Turbine Oil	0	-0.68	0.045	15
Marinus Value Oil	0	-0.68	0.045	15
Mars TLP	0	2.28	0.045	---
Maui	1	-0.14	0.013	11
Maya	0	1.38	0.045	---
Maya crude	0	1.45	0.045	---
Mississippi Canyon Block 194	0	2.62	0.045	---
Mississippi Canyon Block 72	0	2.15	0.045	---
Mississippi Canyon Block 807	0	2.05	0.045	---
Nektroalik	0	0.62	0.045	---
Neptune Spar (Viosca Knoll 826)	0	3.75	0.045	---
Nerlerk	0	2.01	0.045	---

Oil-type	Curve type	A	B	T [°C] >
Ninian	0	2.65	0.045	---
Norman Wells	0	3.11	0.045	---
North Slope - Middle Pipeline	0	2.64	0.045	---
North Slope - Northern Pipeline	0	2.64	0.045	---
North Slope - Southern Pipeline	0	2.47	0.045	---
Nugini	0	1.64	0.045	---
Odoptu	0	4.27	0.045	---
Oriente	0	1.32	0.045	---
Oriente	0	1.57	0.045	---
Orimulsion plus water	0	3	0.045	---
Oseberg	0	2.68	0.045	---
Panuke	0	7.12	0.045	---
Pitas Point	0	7.04	0.045	---
Platform Gail (Sockeye)	0	1.68	0.045	---
Platform Holly	0	1.09	0.045	---
Platform Irene - long term	0	0.74	0.045	---
Platform Irene - short term	1	-0.05	0.013	4
Point Arguello - co-mingled	0	1.43	0.045	---
Point Arguello Heavy	0	0.94	0.045	---
Point Arguello Light	0	2.44	0.045	---
Point Arguello Light -b	0	2.3	0.045	---
Port Hueneme	0	0.3	0.045	---

Oil-type	Curve type	A	B	T [°C] >
Prudhoe Bay (new stock)	0	2.37	0.045	---
Prudhoe Bay (old stock)	0	1.69	0.045	---
Prudhoe stock b	0	1.4	0.045	---
Rangely	0	1.89	0.045	---
Sahara Blend	1	0.001	0.013	---
Sahara Blend - long term	0	1.09	0.045	---
Sakalin	0	4.16	0.045	---
Santa Clara	0	1.63	0.045	---
Scotia Light	0	6.87	0.045	---
Scotia Light	0	6.92	0.045	---
Ship Shoal Block 239	0	2.71	0.045	---
Ship Shoal Block 269	0	3.37	0.045	---
Sockeye	0	2.14	0.045	---
Sockeye co-mingled	0	1.38	0.045	---
Sockeye Sour	0	1.32	0.045	---
Sockeye Sweet	0	2.39	0.045	---
South Louisiana	0	2.39	0.045	---
South Pass Block 60	0	2.91	0.045	---
South Pass Block 67	0	2.17	0.045	---
South Pass Block 93	0	1.5	0.045	---
South Timbalier Block 130	0	2.77	0.045	---
Statfjord	0	2.67	0.06	---
Sumatra Heavy	1	-0.11	0.013	8
Sumatra Light	0	0.96	0.045	---
Taching	1	-0.11	0.013	8
Takula	0	1.95	0.045	---
Tapis	0	3.04	0.045	---
Tchatamba Crude	0	3.8	0.045	---
Terra Nova	0	1.36	0.045	---
Terresso 150	0	-0.68	0.045	15
Terresso 220	0	-0.66	0.045	15
Terresso 46 Industrial oil	0	-0.67	0.045	15
Thevenard Island	0	5.74	0.045	---
Turbine Oil STO 120	0	-0.68	0.045	15
Turbine Oil STO 90	0	-0.68	0.045	15
Udang	1	-0.14	0.013	11
Udang - long term	0	0.06	0.045	---
Vasconia	0	0.84	0.045	---
Viosca Knoll Block 826	0	2.04	0.045	---
Viosca Knoll Block 990	0	3.16	0.045	---
Voltesso 35	1	-0.18	0.013	14
Waxy Light and Heavy	0	1.52	0.045	---
West Delta Block 30 w/water	1	-0.04	0.013	3
West Texas Intermediate	0	2.77	0.045	---
West Texas Intermediate	0	3.08	0.045	---
West Texas Sour	0	2.57	0.045	---

Oil-type	Curve type	A	B	T [°C] >
White Rose	0	1.44	0.045	---
Zaire	0	1.36	0.045	---

Legend

Oil-type:	Common oil name (brand)
Curve type:	logarithmic (0) square root (1)
A, B:	Oil specific evaporation parameters
T [°C] >	Temperature limit [°C]

Please note:

These tables are based on the information provided by Fingas (2004). The parameter 'Curve type' corresponds to model parameter 'evap_type', the specific constants A and B to the model parameters 'evapA' and 'evapB'. Some evaporation equations will not work for ambient water temperatures below the given minimum temperature in °C. Sometimes you find multiple entries for the same oil type. In this case usually a long- and a short-term behaviour are described or the data is based on different sources.

If no oil specific constants are available alternatively the percent evaporated at 180 °C can be used (model parameter 'evap180'). Then a generic evaporation scheme is used. In this case the ambient temperature should not be below 15°C.

APPENDIX C

Sea-bed Blow-out

C Sea-bed Blow-out

The following method for estimating the droplet size based on release conditions is applied in both CDOG and DEEPBLOW. The flow conditions just before the release point is assessed according to the local void ratio[4]:

- Case a: if local void ratio ≤ 0.95, it is an oil jet. In this case, inside the pipe, the continuous phase is the oil phase with dispersed gas bubbles
- Case b: if the local void ratio > 0.95, it is a mist flow. In this case, inside the pipe, the continuous phase is a gas phase with dispersed oil droplets.

C.1 Droplet and bubble sizes

C.1.1 Oil droplets

The size of the oil droplets is calculated though the equations of Johansen et al. (2013):

Variable	Equation	Ref.
Reynolds number	$Re = \frac{\rho \cdot U_C \cdot D}{\mu}$	(C. 1)
Weber number	$We = \frac{\rho \cdot U_C^2 \cdot D}{\sigma}$	(C. 2)
Ohnesorge number	$Oh = \frac{\mu}{\sqrt{\rho \cdot \sigma \cdot D}}$	(C. 3)
Viscosity number	$Vi = \frac{\mu \cdot U}{\sigma}$	(C. 4)
Froude number	$Fr = \frac{U_n}{\sqrt{g' \cdot D}}$	(C. 5)
Effective velocity	$U_n = \frac{U_{oil}}{\sqrt{1-n}}$	(C. 6)
Effective velocity	$U_C = Fr \cdot (1 + \frac{1}{Fr})$	(C. 7)
Modified Weber number	$We' = \frac{We}{1 + \beta \cdot Vi \cdot (\frac{d_{50}}{D})^{\frac{1}{3}}}$	(C. 8)
Modified Weber number scaling	$\frac{d_{50}}{D} = A \cdot We'^{\frac{-3}{5}}$	(C. 9)

[4] It has not been possible to find a clear definition of the local void ratio, but it taken as the ratio between the gas volume and the oil volume.

Where

U	exit velocity (m/s)
U_{oil}	oil exit velocity (m/s)
D	diameter (m)
d_{50}	the volume median droplet diameter (m)
ρ	oil density (kg/m^3)
μ	oil dynamic viscosity (kg/m/s)
σ	interfacial tension between oil and water (N/m or kg/s^2)
g'	reduced gravity = $g \cdot(\rho_w - \rho_m)/\rho_w$
g	acceleration of gravity(m/s^2)
ρ_w	density of the ambient water (kg/m^3)
ρ_m	density of the mixture of oil and gas at the exit (bubbly jet).

A and B are empirical coefficients that was determined as A = 15.0 and B = 0.8

The modified Weber number scaling accounts for the effect of viscos forces on the breakup of droplets. Note that the equation is implicit in d50 and that an iterative procedure is required to solve it.

Knowing the d_{50}, the droplet size distribution is computed from the Rosin-Rammler-type distribution. This implies that the fraction of the total oil volume contained in droplets with diameter less than d is given by:

$$V(d) = 1 - \exp(-0.693 \cdot (\frac{d}{d_{50}})^{1.8} \quad \text{(C. 10)}$$

C.1.2 Gas bubble size

The initial diameter of the gas bubble is set at 0.005 m. This diameter will increase as the bubble rises vertically and the ambient pressure decreases. The bubble may even become so large so it splits into two or more bubbles. This is however not accounted for in DHI's Oil Spill Model.

C.2 Vertical bubble velociy

Several equations for the calculation of terminal velocity of the bubbles in dependence of the size and shape of the gas bubbles have been suggested, e.g. Zheng & Yapa (2003), Johansen 2000) - see Table C. 1. The equations suggested by Johansen (2000) are used in the DHI's Oil Spill model.

Table C. 1 Estimation of Ububble (m/s)

Size, shape	**CDOG** (Zheng & Yapa, 2003)	**DEEPBLOW** Ububble (Johansen, 2000)
< 5 mm, spherical	$U_{bubble} = \frac{Re \cdot \mu}{\delta_{EG} \cdot \rho}$	$U_{bubble} = \frac{1}{\frac{1}{U_{bubble_1}} + \frac{1}{U_{bubble_2}}}$ $U_{bubble_i} = \sqrt{\frac{4 \cdot g' \cdot \delta_{EG}}{3 \cdot C_{D,i}}}$ $C_{D,1} = \frac{24}{Re}$ $C_{D,2} = 0.44$ $g' = g \cdot \frac{\rho_a - \rho_g}{\rho_a}$
≈5-13 mm, ellipsoidal	$U_{bubble} = \frac{\mu}{\delta_{EG} \cdot \rho} \cdot M^{-0.149} \cdot (J - 0.857)$ $J = 0.94 \cdot H^{0.757}, 2 < H < 59.3$ $J = 3.42 \cdot H^{-0.149}, H \geq 59.3$ $H = \frac{4}{3} \cdot E_0 \cdot M^{-0.149} \cdot \left[\frac{\mu}{\mu_w}\right]^{-0.14}$ $M = \frac{g \cdot \mu^4 \cdot \Delta\rho}{\rho_a{}^2 \cdot \sigma^3}$ $E_0 = \frac{g \cdot \Delta\rho \cdot \delta_{EG}^2}{\sigma}$	
>≈13 mm, spherical cap	$U_{bubble} = 0.711 \sqrt{g \cdot \delta_{EG,c} \cdot \frac{\Delta\rho}{\rho_a}}$ $\delta_{EG,c} = 0.015\ m$	

Where

DG→L: molecular diffusivity of a gas in a liquid (cm^2/s)

δ_{EG} equivalent diameter of bubbles (cm). The diameter will increase with decrease in pressure and decrease if gas is removed due to dissolution and/or hydrate formation.

Ububble terminal velocity (cm/s)

C.3 Dissolution

C.3.1 Dissolution of oil components

The dissolution of oil components from oil droplets is modelled by the same equations as the dissolution from the surface slick, where the slick area is replaced by the total droplet surface area. The droplet sizes and thus the surface area will decrease due to removal of substances by dissolution. An excel sheet has been developed, where the total surface of the oil droplets is calculated (A0) (expressed as m2/m3 oil spilled) in dependence of spill conditions. Furthermore, the total number of oil droplets (number per m^3) $n_{droplet}$ is calculated. The total area is then assumed to decrease linearly as a function of "degree" of dissolution (f).

The average diameter at neutral buoyancy, where the plume is assumed to split up in gas bubbles and oil droplets is calculated from (d_{avg}):

$$d_{avg} = \sqrt{\frac{A_0 \cdot (1 - f)}{\pi \cdot n_{droplet}}} \quad \text{(C. 11)}$$

C.3.2 Dissolution of gas

The dissolution rate of gas into sea water is described by (e.g. Zheng & Yapa 2002):

$$\frac{dn}{dt} = K \cdot A \cdot (C_s - C_0) \qquad \text{(C. 12)}$$

Where

K	is the mass transfer coefficient (m/d)
A	is the surface area of the gas bubble (m^2)
C_S	is the solubility of the gas ($mole/m^3$)
C_0	is the actual concentration of dissolved gas in the sea water (is set to 0) ($mole/m^3$)

K depends on the size and shape of the bubbles. Table C. 2. The below equations are used in the DHI model.

Table C. 2 Estimation of K (cm/d)

Size, shape	**CDOG** (Zheng & Yapa, 2003)
< 5 mm, spherical	$K = 976.32 \cdot \sqrt{\frac{U_{bubble} \cdot D_{G\to L}}{0.45 + 0.2 \cdot \delta_{EG}}}$
≈5-13 mm, ellipsoidal	$K = 5616 \cdot \sqrt{D_{G\to L}}$
>≈13 mm, spherical cap	$K = 5996 \cdot \frac{\sqrt{D_{G\to L}}}{\sqrt[4]{\delta_{EG}}}$.

C.3.3 Gas solubility

The solubilty of a gas is strongly depending on salinity, temperature, and pressure. The solubility dependency is calculated from (Zheng et al., 2002):

$$f_G = H^* \cdot x_l \cdot \exp\left(\frac{P \cdot v_l}{R \cdot T}\right) \qquad \text{(C. 13)}$$

Where

v_l	is the molar volume of the gas in dissolution ($33 \cdot 10^{-6}$ $m^3/mole$ and $36.5 \cdot 10^{-6}$ $m^3/mole$ for CO_2 and CH_4 respectively)
x_l	is the mole fraction of dissolved gas in solution at equilibrium (can readily be "translated" into C_S):

$$C_S\left(\frac{mole}{m^3}\right) = \left(\frac{x_l\left(\frac{mole}{mole}\right) \cdot \rho_{PW}\left(\frac{kg}{m^3}\right)}{18\ \frac{g}{mole} \cdot 10^{-3}\ \frac{kg}{g}}\right) \qquad \text{(C. 14)}$$

H* is the Henrys law constant for the solution of gas in saline water. It depends on temperature and salinity. The following general equation is used to express the Henrys law constant in dependence of salinity and temperature:

$$H^* = H(T^0) \cdot f_{salinity} \cdot \exp\left(\frac{H_B}{R \cdot T^0} - \frac{H_B}{R \cdot T}\right) \quad \text{(C. 15)}$$

Where T is the absolute temperature, $f_{salinity}$ is a factor accounting for the impact of salinity on Henrys law constant. It is 1 for fresh water, and it depends on type of gas for marine water: for example it is appr. 0.85 and 0.8 for CO_2 and CH_4 respectively.

The fugacity of the gas (f_G) (Pa) can be calculated from:

$$f_G = \varphi \cdot p_G \quad \text{(C. 16)}$$

Where

Is the fugacity coefficient of the gas, which can be estimated from:

$$\varphi = \exp\left(\frac{P_r}{T_r} \cdot (B^0 + \omega \cdot B^1)\right) \quad \text{(C. 17)}$$

C.4 Gas density

In deep water with high pressures, gas does not behave as an ideal gas. The solubility of gas depends on ambient pressure, temperature and salinity. Gas bubbles may experience significant variations in sizes and shapes caused by the gas expansion (decrease in pressure) and dissolution.

The PVT-relationship for a gas may be described as:

$$Zc = \frac{P \cdot V}{R \cdot T} \quad \text{(C. 18)}$$

Where

P	is the ambient pressure (Pa) = 101325 Pa + [Depth·Density·g]
V	is the molar volume (m3/mole)
T	is the ambient absolute temperature (K)
Zc	is the so-called compressibility factor, being equal to 1 if an ideal gas.

Several methods exist for calculating Z. The Pitzer equation is:

$$Zc = 1 + \frac{B \cdot P}{R \cdot T} = 1 + \frac{B \cdot P_C}{R \cdot T_C} \cdot \frac{P_r}{T_r} \quad \text{(C. 19)}$$

Where

P_C	is the critical pressure for the gas
T_C	is the critical temperature for the gas
P_r	is the reduced pressure = P/PC
T_r	is the reduced temperature = T/TC

Pitzer proposed a correlation of the form:

$$\frac{B \cdot P_C}{R \cdot T_C} = B^0 + \omega \cdot B^1 \quad \text{(C. 20)}$$

With

ω is the acentric factor of the gas

$$B^0 = 0.083 - \frac{0.422}{T_r^{1.6}} \quad \text{(C. 21)}$$

$$B^1 = 0.139 - \frac{0.172}{T_r^{4.2}} \quad \text{(C. 22)}$$

The molar volume of a gas (V) (m^3/mole) and density (ρ_G) (kg/m3) can then be calculated by

$$V = \frac{R \cdot T}{P} \cdot [1 + \{\left(0.083 - \frac{0.422}{T_r^{1.6}}\right) + \omega \cdot \left(0.139 - \frac{0.172}{T_r^{4.2}}\right)\} \cdot \frac{P_r}{T_r}] \quad \text{(C. 23)}$$

$$\rho_G = \frac{M_G}{1000 \cdot V} \quad \text{(C. 24)}$$

Where

M_G is the molar mass of the gas (g/mole)

In the below figure, the importance of accounting for non-ideality of the gas of methane and CO_2 is shown. We recall, that Z = 1, if the gas is ideal.

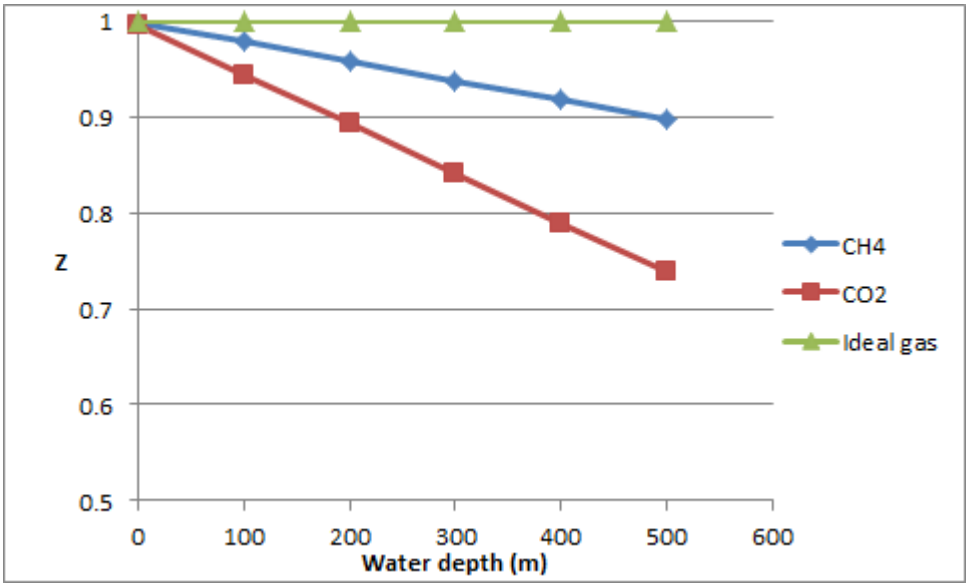

C.5 Hydrate formation

Hydrates are crystalline, non-stoichiometric compounds formed of water and small “guest” molecules. The “guest” molecules are incorporated in cavities of a framework structure of hydrogen-bonded water molecules (“clathrates = cage-forming compounds”).

In natural gas hydrates, methane (CH_4) is the dominating type of guest molecule but other compounds, such as ethane (C_2H_6), propane (C_3H_8), carbon dioxide (CO_2), and hydrogen sulphide (H_2S), may also form stabile hydrate structures at usually high pressure and low temperature conditions. Both, CH_4 and CO_2 form hydrates if the gas or liquid is not significantly contaminated by other possible “guests”. The theoretical unit cell formula of methane-hydrate is: $CH_4 \times 5.75\ H_2O$ with a density of 918.7 kg m^3 and of carbon dioxide hydrate is $CO_2 \times 5.75\ H_2O$ with a density of 1134 kg m^3. However, in natural methane hydrates on average only about 90% of the small cages are occupied by the gas molecule yielding a water/methane ratio of 5.9 (Wikipedia).

As mentioned, gas hydrates are only formed at low temperatures and high pressures. Sloan has prepared a calculation programme calculating the phase equilibria for gas-water systems as a function of temperature and pressure. An example of phase diagram for the methane-water system is shown in Figure C. 1 (based on measured data).

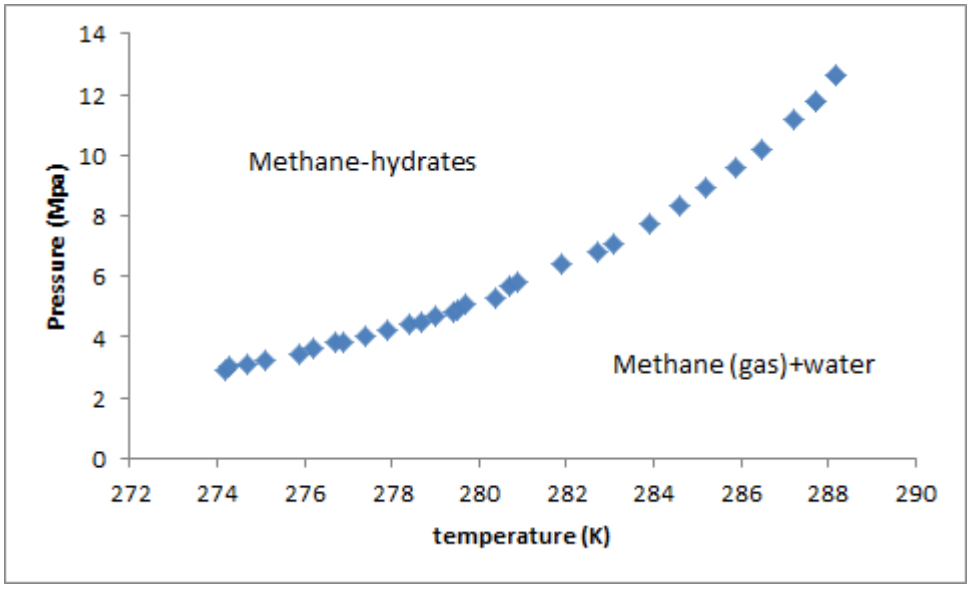

Figure C. 1 Phase system for methane (CH_4) in water

Three processes need to be considered in the modelling of the hydrate formation rate in the gas phase of the jet/plume:

- hydrate kinetics (formation and decomposition),
- mass transfer, i.e. transport of gas for hydrate formation to the point of reaction
- heat transfer, i.e. the transfer of the heat released from hydrate formation around the solid hydrate to change the water temperature

C.6 Water entrainment

Proper estimation of the entrainment is important as it impacts the fate of the plume. CDOG calculates the water entrainment. CDOG applies a quite advanced model developed by Lee and Cheung (1990). The forced entrainment was computed as a sum of shear-induced entrainment and forced entrainment. The latter was computed based on the ambient flow interception in the windward side of the buoyant plume.

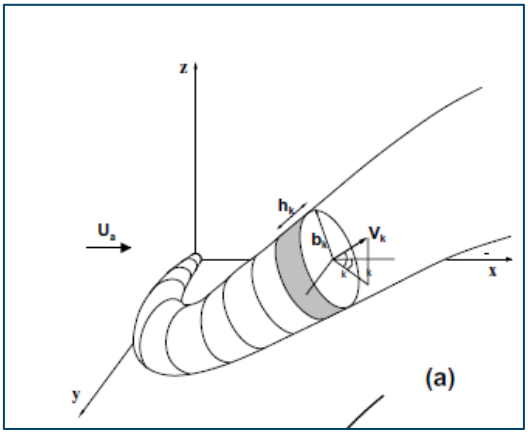

Figure C. 2 Schematic drawing for a buoyant jet

C.6.1 Shear entrainment

$$Q_{Shear}\left(\frac{kg}{d}\right) = A_k \cdot \alpha_s \cdot \Delta U \cdot 24 \cdot 3600 \cdot \rho_a \quad \text{(C. 25)}$$

Where

$$A_k = 2 \cdot \pi \cdot b_k \cdot h^k \quad \text{(C. 26)}$$

α_s is an entrainment factor calculated by:

$$\alpha_s = \sqrt{2} \cdot \frac{0.0057 + \frac{0.554 \cdot \sin\varphi_k}{F_l^2}}{1 + 5 \cdot \frac{V_k}{\Delta U}} \quad \text{(C. 27)}$$

V_k is the jet(plume) velocity (m/s)
ΔU $= |V_k - ua \cdot \cos\varphi_k \cdot \sin\theta_k|$ (m/s)

Where
φ_k is the angle between the jet axis and horizontal plane
θ_k is the angle between the x-axis and the projection of the jet axis on the horizontal plane.
F_l is the local jet densimetric Froude number (Yapa & Zheng, 1977):

$$F_l \cong 2 \cdot \frac{\Delta U}{\sqrt{g \cdot \frac{\Delta\rho \cdot b_k}{\rho_a}}} \quad \text{(C. 28)}$$

C.6.2 Forced entrainment

The forced entrainment is divided up into 3 parts (x, y, z) (uax is the x-component of the ambient current, uay is the y-component of the ambient current, uaz is the z-component of the ambient current) (uax , uay , uaz in m/s):

$$Q_{fx}\left(\frac{kg}{d}\right)=\rho_a \cdot |u_{a,x}| \cdot \left[\pi \cdot b_k \cdot \Delta b_k \cdot |\cos\varphi_k \cdot \cos\theta_k| + 2 \cdot b_k \cdot \Delta s \cdot \sqrt{1-\cos^2\varphi_k \cdot \cos^2\theta_k} + \frac{\pi \cdot b_k^2}{2} \cdot |\Delta(\cos\varphi_k \cdot \cos\theta_{k)}|\right] \cdot 24 * 3600 \quad \text{(C. 29)}$$

$$Q_{fy}\left(\frac{kg}{d}\right) = \rho_a \cdot |u_{a,y}| \cdot \left[\pi \cdot b_k \cdot \Delta b_k \cdot |\cos\varphi_k \cdot \sin\theta_k| + 2 \cdot b_k \cdot \Delta s \cdot \sqrt{1-\cos^2\varphi_k \cdot \sin^2\theta_k} + \frac{\pi \cdot b_k^2}{2} \cdot |\Delta(\cos\varphi_k \cdot \sin\theta_{k)}|\right] \cdot 24 * 3600 \quad \text{(C. 30)}$$

$$Q_{fz}\left(\frac{kg}{d}\right) = \rho_a \cdot |u_{a,z}| \cdot \left[\pi \cdot b_k \cdot \Delta b_k \cdot \sin\varphi_k + 2 \cdot b_k \cdot \Delta s \cdot |\cos\varphi_k| + \frac{\pi \cdot b_k^2}{2} \cdot |\Delta(\sin\varphi_k|\right] \cdot 24 * 3600 \quad \text{(C. 31)}$$

Where

Δs (m) is the displacement of the particle (or control volume) within the time step Δt.

Δbk (m) is the change in radius within the time step Δt (days)

C.7 Gas leakage from a bent plume

If the plume bents then the vertical rising gas bubbles may be released from the plume.

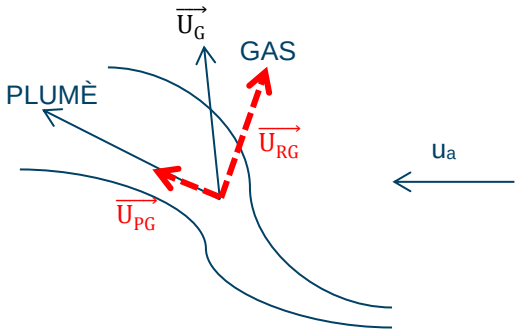

Figure C. 3 Gas may escape as angle is more steep than the plume angle

The gas velocity vector (U) is expressed as a sum of two vectors: one parallel to the plume direction (U_{PG}) and one normal to this (U_{RG}), so

$$\overrightarrow{U_G} = \overrightarrow{U_{PG}} + \overrightarrow{U_{RG}} \quad \text{(C. 32)}$$

$$\overrightarrow{U_G} = \begin{bmatrix} U_{G,x} \\ U_{G,y} \\ U_{G,z} \end{bmatrix} = \begin{bmatrix} u_{a,x} \\ u_{a,y} \\ u_{a,z} + \text{Ububble} \end{bmatrix} \quad \text{(C. 33)}$$

Where
ρ_{Gas} is the density of the gas

$$\rho_{Gas}\left(\frac{kg}{m^3}\right) = \frac{MW_G}{V_G \cdot 1000} \quad \text{(C. 34)}$$

Expressing the plume velocity vector as:

$$\overrightarrow{U_{Plume}} = \begin{bmatrix} U_{Plume,x} \\ U_{Plume,y} \\ U_{Plume,z} \end{bmatrix} \quad \text{(C. 35)}$$

Then $\overrightarrow{U_{PG}}$ can be expressed by

$$\overrightarrow{U_{PG}} = \frac{U_{Plume,x} \cdot U_{G,x} + U_{Plume,y} \cdot U_{G,y} + U_{Plume,z} \cdot U_{G,z}}{U_{Plume,x}^2 + U_{Plume,y}^2 + U_{Plume,z}^2} \cdot \begin{bmatrix} U_{Plume,x} \\ U_{Plume,y} \\ U_{Plume,z} \end{bmatrix} \quad \text{(C. 36)}$$

And therefore, $\overrightarrow{U_{RG}}$ can then readily be found from by:

$$\overrightarrow{U_{RG}} = \overrightarrow{U_G} - \overrightarrow{U_{PG}} \quad \text{(C. 37)}$$

Criteria for that gas may leak (all three criteria should be fulfilled):

- the vertical distance travelled by the plume (z) should be > Z_{sm}
  Z_{sm}= [M_{plume}(initial)×U (initial]^{½}/u_a
- Z_{sm} is set as a constant in the MIKE ECO Lab template.
- The angle (measured from a horizontal plane) at which the gas will move immediately after escaping from the main plume ($\varphi_{k,G}$) shall be steeper than the angle of plume (=φ_k).
  $\left|\overrightarrow{U_{RG}}\right| > \frac{db}{dt}$ (m/s)

Assuming that the Lagrangian particles in the plume element is well mixed, the average amount of gas escaping the particle due to leaking within a time step (mole/s per particle) is calculated in a similar way as DEEPBLOW:

$$\text{Gas leaked} = \frac{G \cdot \frac{2 \cdot (|\overrightarrow{U_{RG}}| - \frac{db}{dt})}{\pi \cdot b}}{N_{particle}} \quad \text{(C. 38)}$$

C.8 Heat balance

The temperature difference between sea bottom and sea surface may be significant > 15°C. As the plume can rise very quickly, it may be relevant to calculate the temperature of the plume on the basis of a heat balance. Heat is released during formation of hydrates, and heat is consumed during decomposition

The heat balance is formulated as follows for the Lagrange particle:

$$M_{Plume} * C_{p,Plume} \frac{dT}{dt} = Hydrate\ formation * \Delta H_{Hydrate} - PW_{entrained} * C_{p,H_2O} * T_{H_2O} \quad \text{(C. 39)}$$

Where

$\Delta H_{Hydrate}$ is the latent heat of hydrate formation (J/mole)

$C_{p,plume}$ is the overall specific heat capacity of the plume (neglecting the heat capacity of the gas) (J/kg/°C):

$$C_{p,Plume} = \frac{M_1 \cdot C_{p,1} + M_2 \cdot C_{p,2} + M_3 \cdot C_{p,3} + PW \cdot C_{p,H2O} + M_{Hydrate} \cdot C_{p,hydrate}}{M_1 + M_2 + M_3 + PW + M_{Hydrate}} \quad \text{(C. 40)}$$

With

$$M_{Hydrate} = (MW_G + MW_{H2O} \cdot n_H) \cdot \frac{G_H}{1000} \quad \text{(C. 41)}$$

Where

$C_{p,i}$ is the specific heat capacity of oil fraction i (J/kg/°C)

C_{H2O} is the specific heat capacity of water (J/kg/°C)

$C_{p,hydrate}$ is the specific heat capacity of the hydrate (J/kg/°C)

C.9 Simulating a seabed blowout

When simulating a seabed blowout the movement and the process involved with the oil/gas jet are calculated with a much finer internal sub time step than the other parts of the simulation. In order to be able to properly resolve the spatial/temporal aspects the user has to specify the ambient conditions at the blowout location and in the water column above. The ambient conditions comprise the velocity components (u,v) and the temperature(t) and salinity (s). The conditions have to be provided via a vertical profile of the water column as a dfs1 file. The name of the file must be “Jet_ambient_uvts.dfs1”. For all practical reasons the vertical profile can be provided in the water column directly above the blow out location. The dfs1 file can be generated using the 3-D metocean result file using the data extraction facility in MIKE zero (the dxfm extraction tool).

In addition, the following parameters have to be provided:

Under constants in the “Eulerian section”:

- Nparticles per time step: Number of particles released in each time step. To be provided again under “Particle Sources”
- Z0: start vertical position of blow out: The depth elevation at which the blow out occur. It is important that the elevation provide is correct relative to the bathymetry in the mesh file. It is recommended to use an elevation slightly above the seabed to avoid immediate “sedimentation of released particles.
- D0: efflux diameter: The diameter of the circular well blow out hole. To be provided again under “Particle Sources”

Under particle sources:

- theta, vertical angle of jet/plume (deg. from horiz.) : Initial vertical angle of the jet
- sigma, horizontal angle of jet/plume (anti-clockwise from East)): Initial vertical angle of the jet
- m, momentum flux of jet/plume (m4/s2): Initial momentum flux of the jet (combined, oil, gas, water momentum flux)
- q, volume flux of jet/plume (m3/s): Initial volume of the jet (combined, oil, gas, water volume flux)
- r, density of jet/plume (kg/m3): Initial density of the plume (combined, oil, gas, water density)
- t, temperature of jet/plume (K): Initial temperature of the plume (combined, oil, gas, water temperature)
- s, salinity of water content in jet/plume (PSU): Initial salinity of water in the plume
- DSBO, switch for deep sea blow out (1: jet/plume, 0: far-field): A switch indicating sub sea blow out using a jet formulation (DSBO = 1)
- DSBO_2, switch for deep sea blow out-release level (1/0) : A switch indicating sub sea blow out using a jet formulation (DSBO_2 = 1)
- DSBO_3, switch for deep sea blow out-when particle hits the water surface (1/0) : A switch indicating sub sea blow out using a jet formulation (DSBO_3 = 1)
- Gas (moles): The initial gas flux (moles or moles per second) from the blow out
- GasH (moles): The initial gas hydrate flux (moles or moles per second) from the blow out
- WaterMass in jet/plume (kg) (DSBO=1): The water flux mass (kg or kg per second)
- Nbub, number (in millions) of gas bubbles in jet/plume (no): Initial total number of gas bobbles in the blow out
- Droplet surface area in jet/plume (m2) . Initial total oil droplet area in the blow out
- b_old, old jet/plume width (m): Initial width (diameter) in the jet blow out

APPENDIX D

The GAS Module

D The GAS module

D.1 General

In case of a deep sea blowout large amounts of gas may be released from the oil plume. These gas bubbles ascend to the surface with a characteristic slip velocity, the horizontal position is determined by the surrounding current flow. Bubbles are assigned to one of three regimes after their diameter, small spherical, intermediate ellipsoidal shaped and large cap shaped bubbles. The regime determines the slip velocity and other physical properties as well as the mass transfer coefficient. The volume and mass of a GAS particle changes due to the changing pressure and diffusion of gas. The module provides 9 predefined and one user defined gas type.

D.2 Variables

The GAS module handles particles that become released from the main oil jet and ascend to the surface. Each GAS particle is characterised by some individual variables:

Variable	Description
Volume	Current volume [m3]
Mass	Current gas mass [mole]
Diameter	Characteristic bubble diameter when leaving the jet
Last_temperature	Internal state, last time step temperature

The rate of change in the volume and mass is given as:

Volume:

$$\frac{d\text{Volume}}{\text{dt}} = (\text{PressureChange} - \text{DissolutionVolumeLoss}) \quad \text{(D. 1)}$$

Mass:

$$\frac{d\text{Mass}}{\text{dt}} = -\text{Dissolution} \quad \text{(D. 2)}$$

D.3 Bubble geometry and slip velocity

Characteristic volume and equivalent bubble radius
The characteristic bubble volume is calculated as the equivalent volume and radius of a spherical bubble:

$$BubbleVolume = \frac{4}{3}\pi * \left(\frac{Diameter}{2}\right)^3 \quad \text{(D. 3)}$$

$$R_{eq} = \sqrt[3]{\frac{BubbleVolume * 3}{4\pi}} \quad \text{(D. 4)}$$

D.4 Bubble regime

According to their shape, moving bubble can be assigned to different shape regimes. Small bubbles are spherical. If they become larger, the increasing drag deforms them into ellipsoid, lentil-shaped forms that, when growing even larger, become cap shaped. To differentiate between the regimes the bubble diameter us used and tested against the regime thresholds.
The diameter thresholds are computed after (Zheng and Yapa 2000) and depend on the fluid and gas density, fluid viscosity and surface tension. Typical values for air in water are around the values represented in the next table.

Regime	Diameter threshold (typical)
Spherical	< 1 mm
Ellipsoid	~ 1 mm
Spherical-cap	10.0-16.0 mm

D.5 Terminal bubble velocity

The terminal slip velocity is calculated as described in (Zheng and Yapa 2000). It depends on the bubble regime, (equivalent) diameter, density and viscosity of the ambient fluid and gas bubble.

Regime	Terminal bubble velocity	
Spherical	$U_T = \frac{\mu}{\rho d_e} * R_x$	(D. 5)
Ellipsoid	$U_T = \frac{\mu}{\rho d_e} M^{-0.149}(J_x - 0.857)$	(D. 6)
Spherical-cap	$U_T = 0.711\sqrt{g * d_e * \frac{\Delta\rho}{\rho}}$	(D. 7)

Where

U_T	terminal velocity [cm/s]
d_e	equivalent diameter
μ	dynamic viscosity of ambient fluid
ρ	density of ambient fluid
Δρ	density difference between gas bubble and ambient fluid
R_x	Reynolds number, adjusted for d_e as given by (Zheng and Yapa 2000).
M	Mortens number
J_x	dimensionless group, depends on d_e

D.6 Total surface area

The total surface area is computed as

$$A_{total} = \frac{Volume_{total}}{BubbleVolume} * 4\pi * {R_{eq}}^2 \quad \text{(D. 8)}$$

The $Volume_{total}$ is the total swarm volume whereas *BubbleVolume* and R_{eq} are the volume and radius of a characteristic bubble.

Constants:
All GAS particles share a common set of constants, describing the GAS type in more details

Constant	Description
GasType	Gas Type [0-9], see below
UseDiffusion	Switch to enable/disable mass loss due diffusion
Density	Gas density at standard conditions [kg/m³], if not derived from gas type
MolarVolume	Molar volume [m³/mole], if not derived from gas type
CriticalTemperature	Critical temperature [deg.C] , if not derived from gas type
CriticalPressure	Critical pressure [bar] , if not derived from gas type

D.7 Generic gas types

To compute some of the internal characteristics, 9 different predefined gas types are available. **Please note that you have to give the proper density and molar** volume **in the constants.**

Type	Description	Sum formula
0	Ideal gas	-
1	Nitrogen	N_2
2	Carbon dioxide	CO_2
3	Methane	CH_4
4	Ethane	C_2H_6
5	Propane	C_3H_8
6	IsoButante	C_4H_{10}
7	nButane	C_4H_{10}
8	Hydrogen sulfide	H_2S
9	User defined	-

D.8 Gas density

Type	Description	Density [kg/m3][5]
0	Ideal gas	1
1	Nitrogen	1.1848
2	Carbon dioxide	1.8714
3	Methane	0.6797
4	Ethane	1.2822
5	Propane	1.8988
6	IsoButante	2.5326
7	nButane	2.5436
8	Hydrogen sulfide	1.4534
9	User defined	1.3540

From: Air Liquide Gas Encyclopedia, http://encyclopedia.airliquide.com/Encyclopedia.asp

[5] Under standard conditions, 15°C 1013 hPa

D.9 Gas molecular weight

Type	Description	Molar weight [kg/mole]
0	Ideal gas	22.414 * 10^{-3}
1	Nitrogen	28.013 * 10^{-3}
2	Carbon dioxide	44.010 * 10^{-3}
3	Methane	16.043 * 10^{-3}
4	Ethane	30.069 * 10^{-3}
5	Propane	44.096 * 10^{-3}
6	IsoButante	58.122 * 10^{-3}
7	nButane	58.122 * 10^{-3}
8	Hydrogen sulfide	34.081 * 10^{-3}
9	User defined	31.999 * 10^{-3}

From: Air Liquide Gas Encyclopedia, http://encyclopedia.airliquide.com/Encyclopedia.asp

D.10 Volume change

The volume of a gas bubble changes due to the change in pressure and the diffusion loss when gas bubbles move vertical in the water column.

D.10.1 Pressure change caused volume change

The change is calculated as the relative volume change rate do to different pressure and temperature

$$PresureChange = Volume * (ChangeFactor(Gastype, T_{old}, P_{old}, T_{new}, P_{new}) - 1) * \frac{86400}{dt} \quad \text{(D. 9)}$$

Where *ChangeFactor* is the relative volume change computed according to Boyle's law. It dependent on the specific gas type, the current and previous pressure (depth) and temperature ([K]) as:

$$ChangeFactor = \left(Z_{new} * \frac{T_{new}}{P_{new}}\right) \Big/ \left(Z_{old} * \frac{T_{old}}{P_{old}}\right) \quad \text{(D. 10)}$$

The pressure at a certain depth below the surface is calculated as:

$$P[Pa] = 101325.0 + (depth[m] * \rho_w * g) \quad \text{(D. 11)}$$

(with $\rho_{w\ being\ the}$ ambient density e.g. ρ_w(35 PSU, 1°C)= 1028.0941 kg/m³, g=9.81 m/s²) *Z* is the compressibility factor of the gas at given pressure and temperature. For ideal gas Z is defined as:

$$Z = \frac{PV_m}{RT} \quad \text{(D. 12)}$$

(P=pressure, V_m=molar volume, R=gas constant, T=Temperauter K). The GAS module supports two methods to calculate the compressibility Z for real gas specie (see below for details)

Method	Ref
1 (default)	Using second virial coefficients after (Pitzer and Curl 1957)
2	(Redlich and Kwong 1949)

If e.g. a bubble of ideal gas (Z=1) raises from a depth of 90 m (P_{90}~1009029 Pa) to 50 m (P_{50}~605605.2 Pa) in constant temperature T=10°C=283.15 K the change factor is:

$$ChangeFactor = \left(1 * \frac{283.15}{605605.2}\right) \Big/ \left(1 * \frac{283.15}{1009029}\right) = \frac{1009029}{605605.2} \sim 1.66 \quad \text{(D. 13)}$$

i.e. the volume increases about 66%.

D.10.2 Dissolution / diffusion

Gas diffuses in and out through the bubble walls. The direction of the net transfer is actually decided by the difference of the partial pressures inside and outside the bubbles. Here we assume that there is just a net outflow, i.e. we assume a constant partial pressure of 0.0 in the ambient water. Thus the equation describing the diffusion is

$$Dissolution = Mass * DiffusionRate * \frac{86400}{dt} \quad \text{(D. 14)}$$

$$DiffusionRate = K_{total} * A_{total} * (C_{sat} - C_0) \quad \text{(D. 15)}$$

K_{total} is the mass diffusion coefficient, A_{total} the total surface area of the bubble (swarm) and C_{sat} the saturation coefficient of the gas at a given temperature and pressure (the ambient concentration C_0 is assumed to be C_0=*0.0*). The diffusibility of the bubble wall may be affected by the pressure and probable forming of a hydrate hull but later effect is not covered by the current model.

Saturation concentration / solubility of gas in water

The solubility or saturation concentration C_{sat} of a gas is calculated as in (Zheng and Yapa 2002) using the modified form of Henry's law based on the assumption:

$$C_S \approx \frac{x^1 \rho_f}{M_f} \quad \text{(D. 16)}$$

Where ρ_f is the density [kg/m³] and M_f the molecular weight [kg/mol] of the fluid and x^1 the mole fraction of dissolved gas in equilibrium condition as given by Henry's law:

$$P = Hx^1 \quad \text{(D. 17)}$$

(H Henry's law constant). Using the fugacity f^g [Pa]

$$f^g = Hx^1 e^{\left(\frac{P\bar{v}}{RT}\right)} \quad \text{(D. 18)}$$

($\bar{v}$=**partial** molar volume [m³/mol]) the saturation concentration is calculated as

$$C_S \approx x^1 * \frac{\rho_f}{M_f} \quad \text{(D. 19)}$$

$$x^1 = \frac{P * f_g}{H * e^{\left(\frac{P\bar{v}}{RT}\right)}} \quad \text{(D. 20)}$$

With ρ_f and M_f being the density and molar weight of the solvent (here water, i.e. $\rho_f = 18.0 \left[\frac{g}{mol}\right]$ and $M_f = 10^6 \left[\frac{g}{m^3}\right]$)

D.10.3 Fugacity coefficient

The fugacity coefficient is calculated as

$$f_g = e^{(Z_{Pitzer}-1)} \quad \text{(D. 21)}$$

Partial molar volumes

The partial molar volumes $\bar{v}$ are approximated from the Air Liquide database.

Type	Description	Partial molar volumes [m3/mol]
0	Ideal gas	$1.00 * 10^{-4}$
1	Nitrogen	$1.62 * 10^{-4}$
2	Carbon dioxide	$1.66 * 10^{-4}$
3	Methane	$1.29 * 10^{-4}$
4	Ethane	$1.04 * 10^{-4}$
5	Propane	$0.84 * 10^{-4}$
6	IsoButante	$0.86 * 10^{-4}$
7	nButane	$0.89 * 10^{-4}$
8	Hydrogen sulfide	$1.22 * 10^{-4}$
9	User defined	$1.00 * 10^{-4}$

D.10.4 Mass transfer coefficient

The mass transfer coefficient is computed after (Zheng and Yapa 2002). It is dependent on the bubble regime (i.e. bubble diameter) and gas diffusivity.

Bubble regime	Mass transfer coefficient
Spherical (small size range)	$K = 0.0113 * \sqrt{\frac{UD}{0.45 + 0.2 * d_e}}$
Ellipsoidal shape (intermediate size range)	$K = 0.065 * \sqrt{D}$
Spherical-cap shape (large size range)	$K = 0.0694 * {d_e}^{-\frac{1}{4}} * \sqrt{D}$
	d_e = equivalent diameter [cm] U = terminal bubble velocity [cm/s] D = molecular diffusivity [cm²/s]

Molecular diffusivity

The molecular diffusivity used is

Type	Description	Molar diffusivity [m/d]
0	Ideal gas	$1.00 * 10^{-4}$
1	Nitrogen	$1.62 * 10^{-4}$
2	Carbon dioxide	$1.66 * 10^{-4}$
3	Methane	$1.29 * 10^{-4}$
4	Ethane	$1.04 * 10^{-4}$
5	Propane	$0.84 * 10^{-4}$
6	IsoButante	$0.86 * 10^{-4}$
7	nButane	$0.89 * 10^{-4}$
8	Hydrogen sulfide	$1.22 * 10^{-4}$
9	User defined	$0.20 * 10^{-4}$

Estimated from: Air Liquide Gas Encyclopedia,
http://encyclopedia.airliquide.com/Encyclopedia.asp

Calculation of the compressibility factors

(Redlich and Kwong 1949)	$$P = \frac{RT}{\hat{V} - b} - \frac{a}{\hat{V}(\hat{V} + b)\sqrt{T}}$$ $$\hat{V} = \frac{zRT}{P}$$ Solving qubic equation $$z^3 - z^2 - qz - r = 0$$ $$r = AB$$ $$q = B^2 + B - A$$ $$A = 0.42747 * \left(\frac{P_r}{T_r^{\frac{5}{2}}}\right)$$ $$B = 0.08644 * \left(\frac{P_r}{T_r}\right)$$ $$\Rightarrow z = root\ (f)$$ (note, P_r is in [atm])

second virial coefficients after (Pitzer and Curl 1957)	$Z = Z_0 + \omega Z_1$ $Z_0 = 1 + B_0 * \frac{P_r}{T_r}$ $Z_1 = B_1 * \frac{P_r}{T_r}$ ω= acentric factor of gas $B_0 = 0.083 - 0.422 * \frac{1}{T_r^{1.6}}$ $B_1 = 0.139 - 0.172 * \frac{1}{T_r^{4.2}}$

In these calculations the reduced temperature T_r and pressure P_r are used, i.e. the ratio of the actual to critical temperature/pressure)

$$T_r = \frac{T}{T_c} \; ; \; P_r = \frac{P}{P_c} \qquad \text{(D. 22)}$$

Critical temperatures [°C] and critical pressures [bar]

Type	Description	Critical temperatures [C°]	Critical pressure [bar]
0	Ideal gas	(-272.15)	(1.0)
1	Nitrogen	-146.96	33.96
2	Carbon dioxide	30.98	73.77
3	Methane	-82.59	45.96
4	Ethane	32.17	48.72
5	Propane	96.74	42.51
6	IsoButante	134.66	36.29
7	nButane	151.98	37.96
8	Hydrogen sulfide	99.95	90.0
9	User defined	-118.75 (Ideal gas)	50.43

From: Air Liquide Gas Encyclopedia, http://encyclopedia.airliquide.com/Encyclopedia.asp

Acentric factor is needed to calculate the second virial coefficients

Type	Description	Acentric factor
0	Ideal gas	-5.96779477304E-01[6]
1	Nitrogen	0.04
2	Carbon dioxide	0.225
3	Methane	0.007
4	Ethane	0.091
5	Propane	0.145
6	IsoButante	0.176
7	nButane	0.193
8	Hydrogen sulfide	0.081
9	User defined	0.021

From http://webserver.dmt.upm.es/~isidoro/

[6] Calculated to result in Z=1 @ 20°C

APPENDIX E

Parameterisation Values for Different Oils

E Parameterisation Values for Different Oils

Please note:
The values in the table below are based on the information provided in the DHI Spill Analysis Data Sheets (cf. DHI_SpillAnalysisDataSheets.pdf).

Representative oil type			Light oil	Middle oil, Low aromatics	Middle oil, High aromatics	Medium crude oil	Heavy fuel oil
Source magnitude	State variables	unit					
Weight	Volatile oil fractions	wt%	72.9	30	30	8	7.5
	Heavy oil fractions	wt%	26.09	68.99	68.99	78.3	77.5
	Asphaltene	wt%	0.01	0.01	0.01	11.5	8
	Wax	wt%	1	1	1	2.2	7
Processes	Class constants						
	Schmidt number		2.7	2.7	2.7	2.7	2.7
	Average molecular weight of volatile fraction	g/mol	123	123	116	121	123
	Vapore pressure of volatile fraction (atm)	atm	0.005	0.005	0.006	0.005	0.005
Simple evaporation	Distillation percentage at 180oC	%	22.5	10	10	5	5
Spreading	terminal thickness	m	0.0001	0.0001	0.0001	0.0001	0.0001
Biodegradation	Decay rate, volatile fraction	per day	0.005	0.005	0.005	0.005	0.005
	Decay rate, in-volatile fraction	per day	0	0	0	0	0
Emulsification	Maxiumum water fraction	m3/m3	0.5	0.5	0.5	0.85	0.85
	Kao constant		3.3	3.3	3.3	3.3	3.3
	Kaw constant		200	200	200	200	200
	Emulsion rate	s/m2	2.00E-06	2.00E-06	2.00E-06	2.00E-06	2.00E-06
Buoyancy	Density of oil at 20oC, volatile fraction	kg/m3	789	796	796	813	787
	Density of oil at 20oC, heavy fraction	kg/m3	878	886	886	997	1011
Water solubility	Water solubility, volatile fraction	kg/kg	2.00E-05	2.00E-05	2.00E-05	2.00E-05	2.00E-05
	Water solubility, heavy fraction	kg/kg	2.00E-07	2.00E-07	2.00E-07	2.00E-07	2.00E-07
Volumentric temperature expansion coefficient	Volatile oil fraction	1/oC	0.0007	0.0007	0.0007	0.0007	0.0007
	In-volatile oil fraction	1/oC	0.0007	0.0007	0.0007	0.0007	0.0007
Photooxidation	Decay rate, volatile fraction	per day	0	0	0	0	0
	Decay rate, heavy fraction	per day	0	0	0	0	0
	Light extinction coefficient	1/m	1	1	1	1	1
Dissolution	Dissolution rate, Light fraction	per day	0.4	0.4	0.4	0.4	0.4
	Dissolution rate, heavy fraction	per day	0.4	0.4	0.4	0.4	0.4
Vertical dispersion	Wind speed for wave breaking	m/s	5	5	5	5	5
	Wave energy dissipation rate	J/m3/s	1000	1000	1000	1000	1000

Representative oil type			Light oil	Middle oil, Low aromatics	Middle oil, High aromatics	Medium crude oil	Heavy fuel oil
Vertical limits	Max distance below surface for surface amount	m	0.05	0.05	0.05	0.05	0.05
	Max distance above bed for bottom amount	m	0.05	0.05	0.05	0.05	0.05
Viscosity	Mooney constant		0.25	0.25	0.25	0.7	0.7
	Dynamic oil viscosity at reference temperature	cP	1.62	1.68	1.68	1283	209
	Reference temperature for dynamic oil viscosity	oC	40	40	40	40	50
	Coeff. exponential temperature dependency		-0.136	-0.136	-0.136	-0.136	-0.136
Oil_area	Oil_area growth rate constant	per sec	150	150	150	150	150

APPENDIX F

Calculating Time Step Probabilities

F Calculating Time Step Probabilities

At various places the per-time-step probability has to be given, i.e. as the beach-lock/ stranding probability. If the probability per day is known one can use the following formula to calculate such per-time-step probability:

$$p_{dt} = p_D^{\left(\frac{dt}{86400}\right)} \quad \text{(F. 1)}$$

where

p_{dt}	is the per-time step [s] probability
p_D	is the per-day probability

Note:

If you have a true rate (e.g *r = X [N/day]*) you need to transform it before using the above equation:

$$p_D = 1 + \ln(r) \quad \text{(F. 2)}$$

F.1 MIRA Classes

The OS model include an option to compute oil classes in the Eulerian grid according to the Norwegian MIRA class method. The purpose of the MIRA classes is to quantify damage after an oil spill as function of the amount of oil present in a specific area. For further information and documentation, see (J0dest0l et al., 1996, S0rgärd et al., 1995).